Journal of Hydrology 561 (2018) 160–178

Contents lists available at ScienceDirect

Journal of Hydrology

journal homepage: www.elsevier.com/locate/jhydrol

Research papers

Simulating streamflow in ungauged basins under a changing climate: The importance of landscape characteristics

Claudia Teutschbein[a,*], Thomas Grabs[a], Hjalmar Laudon[b], Reinert H. Karlsen[a], Kevin Bishop[a,c]

[a] Uppsala University, Department of Earth Sciences, Villavägen 16, SE-75236 Uppsala, Sweden
[b] Swedish University of Agricultural Sciences, Department of Forest Ecology and Management, Skogsmarksgrän, SE-90183 Umea, Sweden
[c] Swedish University of Agricultural Sciences, Department of Aquatic Sciences and Assessment, Lennart Hjelms väg 9, SE-75651 Uppsala, Sweden

ARTICLE INFO

This manuscript was handled by Tim R McVicar, Editor-in-Chief, with the assistance of Joshua Larsen, Associate Editor

Keywords:
Hydrological modeling
Streamflow signatures
Climate change
Forest
Clear-cut
Ungauged

ABSTRACT

In this paper we explored how landscape characteristics such as topography, geology, soils and land cover influence the way catchments respond to changing climate conditions. Based on an ensemble of 15 regional climate models bias-corrected with a distribution-mapping approach, present and future streamflow in 14 neighboring and rather similar catchments in Northern Sweden was simulated with the HBV model. We established functional relationships between a range of landscape characteristics and projected changes in streamflow signatures. These were then used to analyze hydrological consequences of physical perturbations in a hypothetically ungauged basin in a climate change context. Our analysis showed a strong connection between the forest cover extent and the sensitivity of different components of a catchment's hydrological regime to changing climate conditions. This emphasizes the need to redefine forestry goals and practices in advance of climate change-related risks and uncertainties.

1. Introduction

Agreement in the science community is wide spread that changing climate conditions in response to increasing atmospheric concentrations of greenhouse gases substantially affect the water cycle (Milly et al., 2005). In the last century, streamflow patterns have undergone profound changes as a consequence of shifts in temperature, atmospheric water vapor and precipitation (IPCC, 2014). A continued warming of oceans and atmosphere in combination with shifting precipitation trends within the next decades (Alexander et al., 2006; IPCC, 2014) will severely perturb regional hydrology towards the end of the 21st century. The available scientific literature on hydrological climate change impacts in different world regions consistently suggests changing amounts of annual river streamflow (Nijssen et al., 2001), shifts in flood peak magnitudes and timing (Hirabayashi et al., 2013) as well as alterations in flow duration curves (Arora and Boer, 2001). Annual streamflow in snow-dominated catchments in mid to higher latitudes is typically projected to increase (Andréasson et al., 2004; Bergström et al., 2001; Graham et al., 2007a; Graham, 2004; Nijssen et al., 2001), while most tropical and mid-latitude basins will likely experience a reduction (Arora and Boer, 2001; Nijssen et al., 2001). But these findings are mostly based on individual catchments (e.g. Graham et al., 2007a) or on comparisons of catchments located in different climate zones (e.g. Bergström et al., 2001 or Nijssen et al., 2001). The question arises as to whether it is reasonable to draw such generalized conclusions in terms of future hydrological changes for ungauged basins within a larger region based on a selection of representative catchment studies. One could argue that nearby catchments within the same climate zone and underlying geology should function in similar ways, which means that conclusions can be drawn for nearby ungauged basins with the same climate and geological conditions. On the one hand, this hypothesis is supported by the fact that spatial proximity has been found to be a good indicator of catchment similarity (Carey et al., 2010; Sawicz et al., 2011), especially in humid runoff-dominated regions (Patil and Stieglitz, 2012). On the other hand, a recent study by Karlsen et al. (2016b) discovered highly variable hydrological functioning of neighboring and rather similar catchments under *current* climate conditions. The authors reasoned that these variations are controlled by different landscape characteristics such as topography, geology, soils and land cover. In fact, it has long been established that principal streamflow-generating processes are not only controlled by external climatic conditions, but also by physical properties (Beven, 2002; Buttle, 1998; Dunne, 1978; Trancoso et al., 2016). A catchment's physical landscape characteristics result from perpetual adaptive ecological, geomorphic and land-forming processes (Sivapalan, 2005). These physical attributes heavily influence – together with external

* Corresponding author.
E-mail address: claudia.teutschbein@geo.uu.se (C. Teutschbein).

https://doi.org/10.1016/j.jhydrol.2018.03.060
Received 9 December 2016; Received in revised form 19 March 2018; Accepted 21 March 2018
Available online 22 March 2018
0022-1694/ © 2018 Elsevier B.V. All rights reserved.

climate conditions - the present-day hydrological functioning as well as the variability at multiple temporal and spatial scales (Wagener et al., 2007). Such relationships between hydrological behavior and the landscape have been confirmed in many different parts of the world by a number of studies, strongly suggesting that surface runoff, infiltration, water retention and snowmelt dynamics in a catchment are controlled by

1) topographic features such as elevation, aspect or slope (Frisbee et al., 2012; Kokkonen and Jakeman, 2002; Peña-Arancibia et al., 2010; Seyfried and Wilcox, 1995; Williams et al., 2009),
2) soil characteristics such as soil types, profiles or depth (Correa et al., 2016; Farmer et al., 2003; Seyfried and Wilcox, 1995; Tetzlaff et al., 2007; Williams et al., 2009),
3) catchment area (Buttle and Eimers, 2009; Lyon et al., 2012; Post and Jakeman, 1999),
4) land use and land cover (Lyon et al., 2012; Ochoa-Tocachi et al., 2016; Schoonover et al., 2006),
5) vegetation type (Brown et al., 2005; Farmer et al., 2003; Ochoa-Tocachi et al., 2016; Seyfried and Wilcox, 1995; Zhang et al., 2001) and
6) geology (Correa et al., 2016; Seyfried and Wilcox, 1995).

Consequently, the hydrological behavior of catchments in the same region with the same stationary climate conditions varies due to catchment-specific landscape characteristics. Teutschbein et al. (2015) took these findings one step further and used a diagnostic approach to demonstrate that neighboring catchments in the boreal region do not respond uniformly to the same change in climate conditions. Similar indications for considerably different streamflow responses to a changing climate across subcatchments were also found for other geographical regions, such as North America (Chang and Jung, 2010), Central Europe (Kunstmann et al., 2004) or East Africa (Musau et al., 2015). This emphasizes the complexity of the interlinkages between changing climate conditions, landscape characteristics and hydrological behavior, which make it difficult to generalize potential impacts on other catchments within a larger region.

We claim that landscape characteristics are not only important under *stationary* climate conditions, but also play a fundamental role for the sensitivity of a catchment to *changing* climate conditions. Further, we hypothesize that it is possible to predict the combined effects of changes in physical catchment and climate conditions on hydrological processes in ungauged basins given that the underlying functional relationships between landscape characteristics and hydrological shifts in a changing climate can be established.

To explore these theories, the following procedure (Fig. 1) was implemented based on a *meso*-scale low-land catchment and its associated, partly nested subcatchments in the boreal region in Northern Sweden: After collecting all required data (step 1), present and future hydrological regimes were simulated with help of a hydrological model (step 2). Streamflow signatures were calculated for both present and future streamflow simulations to identify signature changes (step 3). Using a regionalization approach, these signature changes were then linked to catchment-specific landscape attributes with help of functional relationships (step 4). Thereafter, the identified functional relationships were validated, i.e., tested for their ability to provide information about the change in an hypothetically ungauged nearby catchment with known physical catchment characteristics (step 5). Finally, we created two virtual forest change cases (step 6) and made an attempt to predict the combined influence of landuse and climate change in hypothetically ungauged basins. Such an analysis is critical to understanding how watersheds will hydrologically respond to combined landuse transformations and future climatic perturbations, which directly reflects upon our ability to reliably project future streamflow in ungauged basins.

2. Study site

The Krycklan catchment is located in the boreal region in northern Sweden (Fig. 2). It has been used as an experimental forest for almost an entire century and has served as a basis for water-related research since the 1980's. For a detailed description of the Krycklan Catchment Study (KCS), the reader is referred to Laudon et al. (2013).

The 67.9 km^2 Krycklan catchment is – according to the Köppen-Geiger classification (Kottek et al., 2006) – characterized by a subarctic/boreal climate with persistent seasonal snow cover and soil frost during winters. Annual mean temperature was on average 1.78 °C while the annual precipitation averaged 640 mm during 1981–2010. The study catchment has 18 partly nested subcatchments, of which the 14 gauged ones were used in this study (Fig. 2a). Till and sediment are the two main types of parent material in the catchment (Fig. 2b), with some areas covered by peat at higher elevations. The elevation ranges from 127 to 373 m a.s.l. (Fig. 2c). Krycklan is a typical catchment in the nemo-boreal region with 87% forest cover (Fig. 2d) consisting of Scots pine (*Pinus sylvestris*) (63%), Norway spruce (*Picea abies*) (26%) and Birch (*Betula pubescens*) (10%) (Laudon et al., 2013). Moreover, the catchment includes a few wetlands (9%), open and arable land (3%) as well as lakes (1%).

3. Data

3.1. Landscape characteristics

Landscape characteristics that can potentially influence streamflow

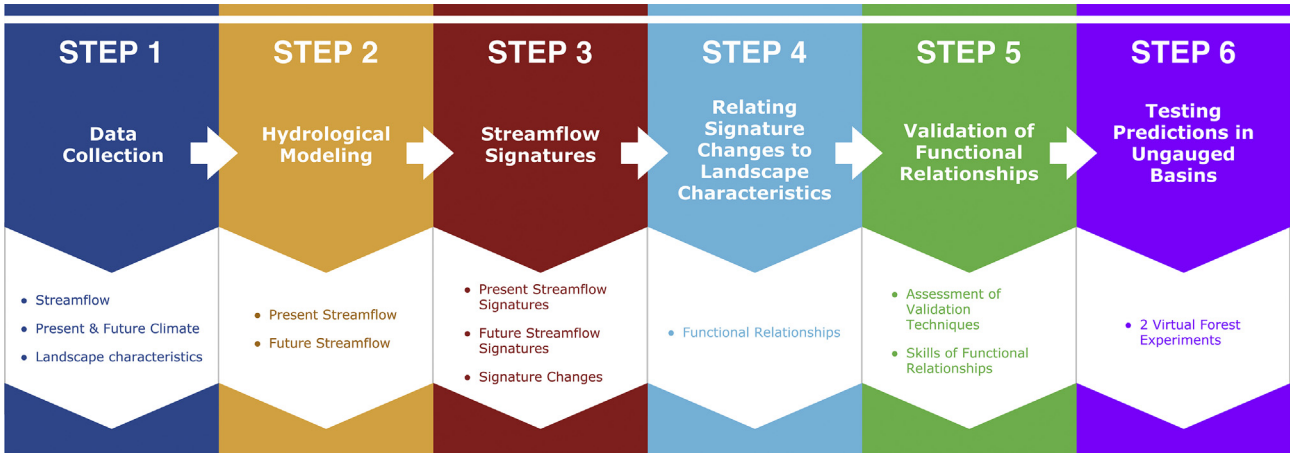

Fig. 1. Roadmap describing the individual steps of the present study.

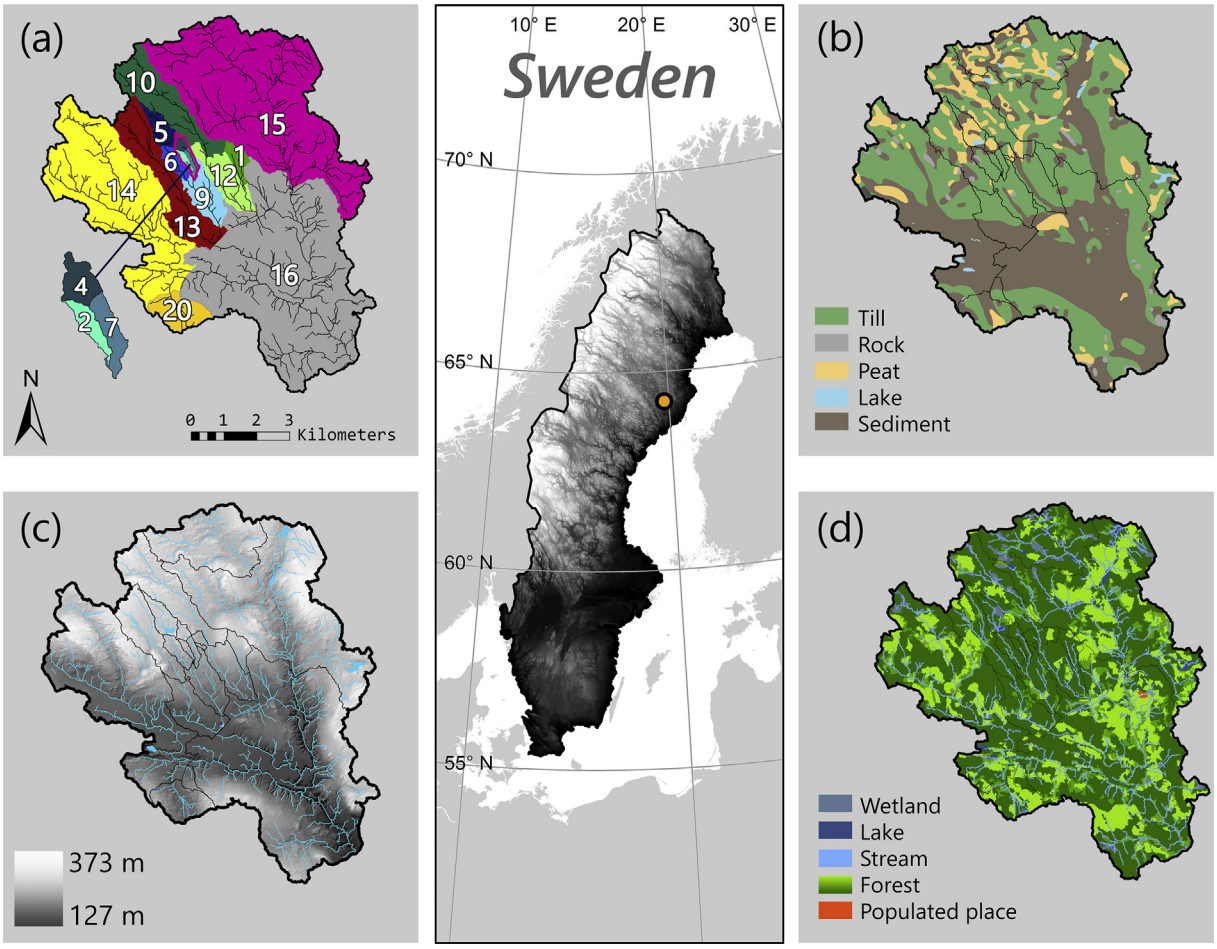

Fig. 2. Location and spatial characteristics of the Swedish Krycklan study catchment and its partly nested subcatchments: (a) location of the subcatchments, (b) geological classifications, (c) topography, and (d) landuse types.

variability in a changing climate are summarized in Table 1 for the entire Krycklan catchment (C16) and its nested subcatchments (C01–C20). Topographic features such as catchment area, elevation above sea level, slope and aspect were calculated from a gridded 2-m digital elevation model (Lantmäteriet Gävle, Sweden). We also included tangential curvature as a measure of flow divergence/convergence (Conrad et al., 2015), elevation above stream (EAS) as an indicator of drainage potential (Laudon et al., 2012) and median subcatchment area (MSCA) as a measure for hillslope and drainage network organization (McGlynn et al., 2003). Geological/soil characteristics were derived from the quaternary deposits map (1:100,000, Geological Survey of Sweden, Uppsala, Sweden) and catchment-specific land cover characteristics from the property map (1:12,500, Lantmäteriet Gävle, Sweden). Forest attributes such as tree species distributions were obtained through professional interpretation of aerial photographs taken in 2004 and 2007 (Persson and Fransson, 2014), while tree biomass was calculated from the 25-m SLU Forest Map 2010, which is based on SPOT 5 satellite data (Dept. of Forest Resource Management, Swedish University of Agricultural Sciences).

Given that five of these characteristics showed only little variation, had rather low percentages or were absent in several subcatchments (i.e., slope, rock, open land, agriculture, lakes), they were excluded from any further analysis. In addition, both wetland area and peat soils were not included in the subsequent analysis, as they both have strong negative correlations with forest cover (Fig. 3a,b) and, thus, contain redundant information. Similarly, spruce and biomass were excluded, because they can be explained by the percentage of birch in the catchments (Fig. 3a,c). Consequently, the remaining 11 catchment characteristics (Table 1, properties written in italic) were chosen for our analysis, because they provide a good representation of the landscape variability in the Krycklan catchment without containing superfluous information.

3.2. Meteorological data

As part of a reference monitoring program, daily air temperature and precipitation were measured directly in the Krycklan catchment following the recommendations from the World Meteorological Organization (WMO) from 1981 to present. The Penman-Monteith model (Monteith, 1965) was used to estimate potential evapotranspiration within the monitoring program using air temperature, humidity, net radiation and wind speed that were also measured directly within the catchment. This model was adjusted to the site using measurements of actual evapotranspiration that were obtained during 1981–1984 with a weighting lysimeter (1 m^3).

3.3. Streamflow data

Daily streamflow in the 14 partly nested catchments has been measured since 2008. With help of pressure transducers (Campbell Scientific Inc., USA), capacitance rods (TruTrack Inc., New Zealand) and radar level sensor (RLS OTT, Germany), water levels were observed continuously during the ice-free season. With the help of heated housings (to avoid ice effects during cold winter months), continuous measurements throughout the entire year were possible at subcatchments C02 (since winter 2011/2012), C04 (since winter 2011/2012),

Table 1
Catchment characteristics of the entire Krycklan catchment (C16, **highlighted**) and its subcatchments sorted by catchment area. Characteristics in italic were selected for further analysis.

Properties	Unit	(Sub)Catchments													
		C02	C04	C01	C07	C05	C06	C20	C09	C10	C12	C13	C14	C15	**C16**
TOPOGRAPHY															
(1) Area	[km^2]	01	0.2	0.5	0.5	0.7	1.1	1.5	2.9	3.4	5.4	7.0	13.8	19.1	**67.9**
(2) Median subcatchment area	[km^2]	0.1	0.2	0.1	0.2	0.7	0.8	1.0	0.3	2.0	1.7	0.5	2.2	0.7	**1.4**
(3) Elevation above sea level	[m]	275	287	279	275	293	282	211	252	297	277	251	229	278	**239**
(4) Elevation above stream	[m]	10.1	9.0	0.9	7.5	2.3	4.2	13.5	4.4	8.3	7.4	6.3	10.2	9.6	**10.0**
(5) Slope[1]	[%]	9	8	9	9	5	9	11	8	10	9	9	12	12	**12**
(6) Tangential curvature	[10^{-4} m^{-1}]	2.8	4.1	0.8	2.8	2.8	2.9	0.8	1.8	2.4	1.8	1.4	0.8	2.3	**1.3**
(7) Aspect	[°]	139	146	177	149	168	164	164	161	161	164	156	171	180	**172**
GEOLOGY/SOIL															
(8) Sediment	[%]	16	27	8	15	30	26	42	20	19	20	29	47	27	**42**
(9) Peat[2]	[%]	0	51	0	19	48	29	12	15	29	19	12	7	15	**9**
(10) Till	[%]	84	22	92	65	16	39	45	62	52	61	57	43	56	**47**
(11) Rock[1]	[%]	0	0	0	0	0	2	2	2	0	0	1	2	1	**1**
LAND COVER															
(12) Wetlands[2]	[%]	0	44	2	18	40	25	10	14	26	17	10	5	15	**9**
(13) Open land[1]	[%]	0	0	0	0	0	0	0	0	0	0	0	1	1	**1**
(14) Agricultural land[1]	[%]	0	0	0	0	0	0	3	0	0	0	1	3	0	**2**
(15) Lakes[1]	[%]	0	0	0	0	6	4	0	1	0	0	1	1	2	**1**
(16) Forest	[%]	100	56	98	82	54	71	88	84	74	83	88	90	82	**87**
FOREST															
(17) Birch	[%]	0	0	2	1	12	4	16	6	12	8	8	10	10	**10**
(18) Spruce[2]	[%]	36	45	63	35	26	26	16	29	21	34	25	23	26	**26**
(19) Pine	[%]	64	55	35	64	62	70	68	65	68	57	68	67	64	**63**
(20) Biomass[2]	[kg/ha]	225	95	180	150	71	103	58	114	77	103	106	75	70	**78**

[1] Excluded due to low variation, i.e. having a range (from minimum to maximum) of less than 10%.
[2] Excluded due to strong significant correlation with other variable (Spearman's rank correlation coefficient ρ_s above +0.8 or below −0.8 at significance level $\alpha = 0.05$).

C05 (since winter 2012/2013) and C07 (since 1981). Measurement sites were either equipped with V-notch weirs, flumes or located at road culverts allowing for fixed and well defined cross sections, or had well defined natural cross sections (e.g., C14, C15 and C16). Rating curves were assessed every year, with more intense gauging during peak flow in spring and low flows in summer. Logger offsets were corrected through manual water height readings at regular intervals. For further details, we refer to Karlsen et al. (2016b). On average, streamflow observations were available for 210 days of the year (streams are closed by a more or less permanent ice cover for the remaining days) and

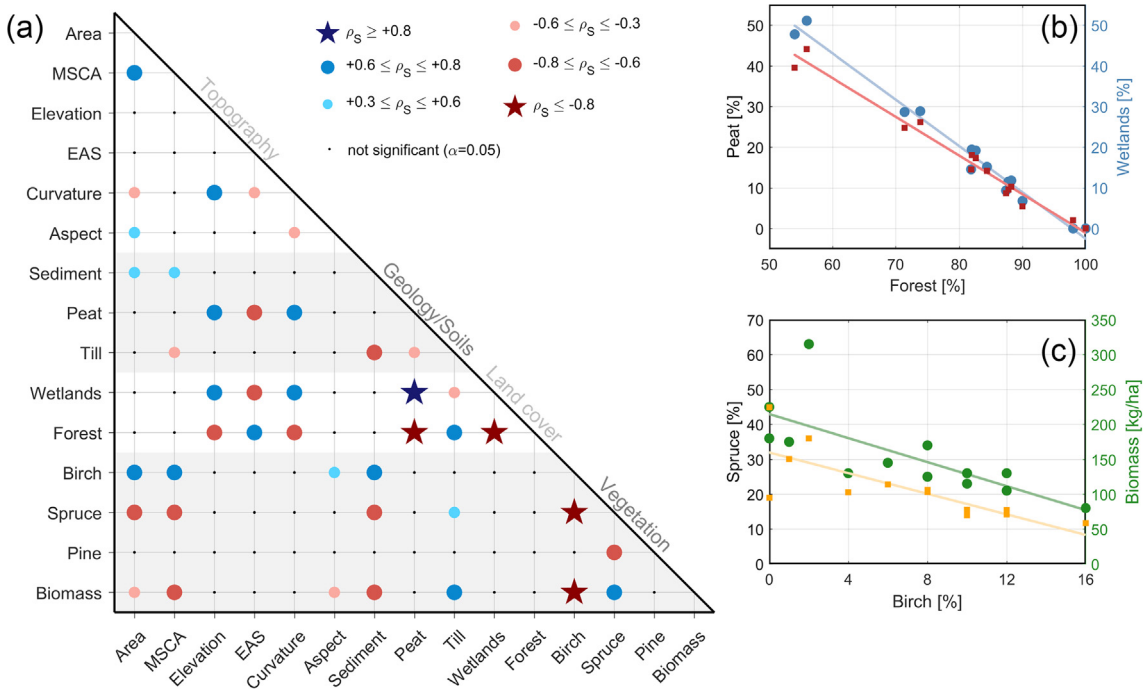

Fig. 3. Spearman rank correlation matrix showing the relationships between selected relevant catchment characteristics of all 14 catchments (a). The linear relationships between strongly correlated variables are also shown: (b) forest versus peat and wetlands, (c) birch versus spruce and biomass.

covered about 80% of the annual flow.

3.4. Current and future climate data

The public database provided by the ENSEMBLES EU project (Van der Linden and Mitchell, 2009) offers 31 transient regional climate model (RCM) simulations forced by various global climate models (GCMs) for download. In this study, we used daily temperature and precipitation simulations for a reference control period (1981–2010) and a future scenario period (2061–2090) from 15 regional climate models (RCMs) that had in common that they were run at a resolution of 25 km × 25 km, had simulations available until year 2100, and assumed the Special Report on Emissions Scenarios (SRES) A1B scenario (Nakicenovic et al., 2000). These climate model simulations were corrected for biases (i.e., systematic errors) to impede the deterioration of subsequent hydrological modeling results (Ehret et al., 2012; Muerth et al., 2013; Teutschbein and Seibert, 2010, 2012, 2013). Here we employed distribution scaling (Boe et al., 2007; Déqué et al., 2007; Ines and Hansen, 2006) to bias-correct daily RCM-simulated temperature and precipitation on a monthly basis. Distribution scaling has proven to be a reliable bias correction method for Swedish catchments under current and future climate conditions (Teutschbein and Seibert, 2012, 2013). It matches the theoretical cumulative distribution function (CDF) of RCM-simulated data with the observed CDF. For a more detailed mathematical description of the procedure we refer the reader to Teutschbein and Seibert (2012).

4. Methods

4.1. Hydrological modeling

4.1.1. The HBV model

The conceptual rainfall-runoff model HBV (Bergström, 1976), which has been used in more than 90 countries and in various versions throughout the years (Bergström and Lindström, 2015), was used to simulate daily streamflow in the individual catchments. More specifically, we employed the HBV-light software package (Seibert and Vis, 2012), which was driven by daily temperature, daily precipitation and long-term monthly mean values of potential evaporation (pET). HBV-light is a lumped model composed of different subroutines that determine snow, soil moisture, evapotranspiration, groundwater, and channel routing, respectively. For further detailed information about HBV, please refer to papers on its model structure and parameter uncertainty (Bergström, 1976, 1992; Bergström and Lindström, 2015; Harlin and Kung, 1992; Lindström et al., 1997; Seibert, 1999).

4.1.2. Calibration and validation

The twelve lumped parameters (Table 2) that regulate HBV's subroutines were calibrated to observed streamflow (2008–2013) separately for each catchment, using the same observed temperature, precipitation and potential evapotranspiration data from the earlier described reference monitoring program. One hundred different optimal parameter sets were obtained through hundredfold calibration with a built-in Genetic Algorithm and Powell optimization (GAP) function (Seibert, 2000) to include parameter uncertainty.

Site C07 was the only site with continuous streamflow observations since 1981, which enabled us to perform an actual split-sample calibration-validation procedure (Klemeš, 1986) by calibrating HBV for the period 2008–2013 and validating the optimized parameter sets for the randomly chosen 10-year period 1991–2000. To evaluate the goodness of fit, Nash-Sutcliffe efficiency (R_{eff}) (Nash and Sutcliffe, 1970), Nash-Sutcliffe efficiency with logarithmic values (L_{eff}) and volume error (VE) were weighted (75%, 20% and 5%, respectively) and combined to a fuzzy measure (X), which was computed at daily time steps following the recommendations by Seibert et al. (1997). For more details on this procedure, we refer to Teutschbein et al. (2015). To further explore the HBV model performance, we created a Taylor diagram (Taylor, 2001), which graphically summarizes the match of simulated and observed streamflow patterns for all subcatchments in terms of their correlation (r), their centered root-mean square difference (RMSD) and their standard deviations (σ_{obs}, σ_{sim}). Because the observed streamflow variability is different for each catchment, these statistics have to be non-dimensionalized before the different catchments can be compared on the same graph (Taylor, 2001). Therefore, RMSD, σ_{obs} and σ_{sim} have to be normalized (indicated by *) by the standard deviation of the corresponding observations (σ_{sim}), which does not change the correlation coefficient and results in a normalized diagram (Taylor, 2001):

$$RMSD^* = \frac{RMSD}{\sigma_{obs}} \quad (1)$$

$$\sigma^*_{sim} = \frac{\sigma_{sim}}{\sigma_{obs}} \quad (2)$$

$$\sigma^*_{obs} = \frac{\sigma_{obs}}{\sigma_{obs}} = 1 \quad (3)$$

4.1.3. Streamflow simulations

After the calibration-validation procedure, the optimized parameter sets were used to model daily streamflow for a reference climate period (1981–2010) and a future period (2061–2090) using the bias-corrected precipitation and temperature series from 15 RCMs as input. Potential evapotranspiration, which is also a required input variable to HBV, was calculated for each RCM with the Hamon equation (Xu and Singh, 2001) based on RCM-simulated temperature:

$$pET = c_1 \cdot \left(\frac{l_d}{12}\right)^2 \cdot \rho_t \cdot 25.4 \text{ with } \rho_t = \frac{4.95}{100} \cdot e^{(c_2 \cdot T)},\ c_1 = 0.69,\ c_2 = 0.055 \quad (4)$$

where pET is potential evapotranspiration in mm/d, c_1 and c_2 are calibrated constants, l_d is the daily daylight length in hours, 25.4 is a factor to convert pET from inch/d to mm/d, ρ_t is a saturated water vapor density term based on RCM-simulated air temperature T. Constants c_1 and c_2 were calibrated so that RCM-specific pET calculated based on Eq. (4) matched the available site-specific Penman-Monteith potential evapotranspiration (see 3.1. Meteorological Data).

By combining an ensemble of 100 optimal HBV parameter sets with an ensemble of 15 RCMs, we covered a more realistic range of uncertainties in climate model structures and in hydrological model parameterization for each 30-yr time period (1981–2010 vs. 2061–2090), for which we assumed the ensemble median to fit observations better than individual streamflow simulations (Teutschbein and Seibert, 2010). The first year of each 30-yr period was neglected as the warm-up period of the HBV-light model. Therefore, we obtained 1500 streamflow simulations of 29 years each, which provided us with 43,500 annual streamflow series for the reference period and 43,500 for the future period (in total 87,000 annual streamflow series) for each catchment.

4.2. Streamflow signature analysis

Streamflow was evaluated in terms of signatures (S) that represent dynamic catchment functioning (Gupta et al., 2008; Wagener et al., 2007), quantify the hydrological responses (Toth, 2013) and are characteristic of a specific catchment (Yadav et al., 2007). Initially, such signatures had been developed for testing and improving hydrological models (Yilmaz et al., 2008), but have in the past also proven useful for determining how streamflow and aquatic communities relate (Pool et al., 2017) as well as for assessing a model's ability to reliably simulate hydrological systems under conditions different from those used for calibration, for instance in a changing climate (Mendoza et al., 2015; Stahl et al., 2011).

The literature provides a wide range of possible streamflow signatures (Clausen and Biggs, 2000; Ley et al., 2011; Shamir et al., 2005;

Table 2
Overview of calibrated HBV model parameters (based on Seibert (1999) and Seibert and Vis (2012)).

Routine	Parameter	Description	Ranges used in calibration
Snow routine	TT	Threshold temperature, which controls the snow accumulation, melting and refreezing.	−2.0 … +1.0 °C
	CFMAX	Degree-day factor	0.5 … 4.0 mm/d/°C
	SFCF	Snowfall correction factor, which compensates for the fact, that evaporation of snow is not simulated by HBV (Seibert, 1999).	0.4 … 0.9 [–]
Soil routine	FC	Maximum of soil moisture storage capacity, which varies with soil types, which are strongly correlated to land use.	50 … 550 mm
	LP	Threshold for potential evaporation (pET), above which all pET from the soil box actually evaporates, while a linear reduction is used otherwise.	0.3 … 1.0 [–]
	BETA	Shape coefficient, which determines the relative contribution from rain and snowmelt to runoff at a given soil moisture deficit.	1.0 … 5.0 [–]
Groundwater routine	PERC	Maximum water flow from upper (groundwater) to lower box (lakes).	0.0 … 4.0 mm/d
	K0	Recession coefficient, changes the recession slope of high flows (Seibert, 2005).	0.1 … 0.99 d^{-1}
	K1	Recession coefficient (upper box), changes the recession slope of intermediate flows (Seibert, 2005).	0.01 … 0.5 d^{-1}
	K2	Recession coefficient (lower box), changes the recession slope of baseflows (Seibert, 2005).	0.00005 … 0.1 d^{-1}
	UZL	Storage threshold	0 … 150 mm
Routing routine	MAXBAS	Routing parameter that defines a triangular weighting function which smoothes the simulated runoff.	1.0 … 2.5 d

Table 3
Overview of 26 streamflow signatures, which were largely based on signature listings by Clausen and Biggs (2000), Shamir et al. (2005), Yadav et al. (2007), Yilmaz et al. (2008) and Ley et al. (2011).

Abbr.	Signature	Calculation
1 (a) Hydrograph (streamflow)		
1)–5) FMean	Mean streamflow (annual or seasonal)	$FMean_{ANN/DJF/MAM/JJA/SON} = mean(Q) = \frac{\sum_{i=1}^{N} Q_i}{N}$, where Q_i is daily streamflow for days i = 1, 2, … N within a specific year (ANN) or a specific season (DJF = winter, MAM = spring, JJA = summer, SON = autumn).
1 (b) Hydrograph (baseflow)		
6)–10) BMean	Mean baseflow (annual or seasonal)	$BMean_{ANN/DJF/MAM/JJA/SON} = mean(Q_b) = \frac{\sum_{i=1}^{N} Q_{b,i}}{N}$, where $Q_{b,i}$ is daily baseflow for days i = 1, 2, … N within a specific year (ANN) or a specific season (see definition above).
11)-15) BFI	Baseflow index (annual or seasonal)	$BFI = 100 \cdot \frac{BMean_{ANN/DJF/MAM/JJA/SON}}{FMean_{ANN/DJF/MAM/JJA/SON}}$
1 (c) Hydrograph (spring flood)		
16) SFD	Spring flood duration	$SFD = no.\ of\ days$ (between starting (*SFstart*) and ending (*SFend*) point of the spring flood)
17) SFP_{mag}	Magnitude of flood peak	$SFP_{mag} = \max(Q)$ within the first 6 months of the year
18) SFP_{time}	Timing of flood peak	$SFP_{time} = day\ i$ on which SFP_{mag} occurs; with $1 \leqslant i \leqslant 182$
19) SFV	Total spring flood volume	$SFV = \sum_{i=SFstart}^{SFend} Q_i$
2 (a) Flow duration curve (high flow)		
20) FHS	High-segment flow	$FHS = \frac{\sum_{h=1}^{H} Q_h}{H}$, where $h = 1, 2, \ldots H$ are the flow indices for flows with exceedance probabilities lower than 0.02, H being the maximum flow.
2 (b) Flow duration curve (median flow)		
21) CV	Streamflow variability	$CV = std(Q)/mean(Q)$ where *std* is the standard deviation.
22) FMed	Median streamflow	$FMed = median(Q)$
23) FMS	Mid-segment slope	$FMS = \log(Q_{m1}) – \log(Q_{m2})$, where m_1 and m_2 are the lowest and highest flow exceedance probabilities (0.33 and 0.66 respectively) within the midsegment.
24) FSkew	Streamflow skewness	$FSkew = FMean/FMed$
2 (c) Flow duration curve (low flow)		
25) FLS	Low-segment flow	$FLS = \frac{\sum_{l=1}^{L} Q_l}{L}$, where $l = 1, 2, \ldots L$ are the flow indices for flows with exceedance probabilities between 0.7 and 0.9, L being the minimum flow in the interval.
3 (a) Water Balance		
26) RR	Runoff coefficient	$RR = 100 \cdot \frac{\sum_{i=1}^{N} Q_i}{\sum_{i=1}^{N} P_i}$, with daily streamflow Q_i and daily precipitation P_i for days i = 1, 2, … N.

Yadav et al., 2007; Yilmaz et al., 2008). To describe the overall water balance, the hydrograph (i.e., seasonal and annual flow variability) and flow durations (i.e., frequency and timing of high, mid-segment and low flows), a selection of 26 relevant signatures (Table 3) was used that could easily be derived from available observed and simulated streamflow and precipitation time series. We followed the routine established by Teutschbein et al. (2015) to automatically analyze the set of 87,000 streamflow series for each of the 14 catchments and calculate the corresponding streamflow signatures. This routine defined the *spring flood peak* as the maximum streamflow value within the first 6 months of the year, based on which spring flood peak magnitude (SFP_{mag}) and timing (SFP_{time}) were calculated. *Baseflow* was then separated with an easy-to-implement recursive digital filter originally proposed by Lyne and Hollick (1979), which provides an objective and repeatable baseflow estimate (Nathan and McMahon, 1990; Ladson et al., 2013). This one-parameter filter merely filters out high-frequency signals, which lacks any physical basis (Nathan and McMahon, 1990; Ladson et al., 2013; Chapman, 1991). In the present study, we followed

the standard procedure for the application of the Lyne and Hollick filter that is provided by Ladson et al. (2013). The separated baseflow served as a basis for finding the *starting* and *ending points* of the spring flood so that *spring flood duration* (SFD) and *volume* (SFV) could be calculated. Thereafter, a wide variety of additional hydrologically relevant signatures related to streamflow, baseflow, flow durations and extreme events (Table 3) was computed for the reference period ($S_{1981–2010}$) and the future ($S_{2061–2090}$).

4.3. Relationship between landscape characteristics and hydrological change

4.3.1. Identification of correlations and functional relationships

First, we related the projected streamflow signature changes ($\%\Delta S$) in each catchment to the catchment-specific landscape characteristics using the non-parametric Spearman's rank correlation coefficient ρ_s (Spearman, 1904). Spearman rank correlation was chosen over linear Pearson product-moment correlation (Pearson, 1920) because Spearman assumes only monotony without making prior assumptions about the nature of the relationships (e.g., linear or logarithmic). The correlation coefficient ρ_s was calculated for all 286 possible combinations of the 11 landscape characteristics (Table 1) and the projected relative changes ($\%\Delta S$) in the 26 streamflow signatures (Table 3) based on the 14 catchment-specific observations. For all landscape-signature pairs, which were significantly correlated ($\alpha = 0.05$), we used the principle of regionalization: Functional relationships were established by fitting different two-parametric regression functions (i.e., linear, exponential, power or logarithmic) as suggested by Seibert (1999) to the entire data set, including all 14 catchments.

4.3.2. Validation of functional relationships using Holdout, Leave-one-out and bootstrap method

For the purpose of testing whether the identified functional relationships between landscape characteristics and projected future streamflow changes ($\%\Delta S$) could potentially be used to obtain information about the change in an ungauged nearby catchment with known physical catchments characteristics, an independent data set was needed for validation. Since such independent data was lacking, we made use of the existing 14 observations (i.e., one observation for each catchment) as a basis for defining a calibration and a validation data set. This was done separately for all landscape-signature pairs that were significantly correlated and for which we were able to fit two-parametric regression functions described in the previous section.

To create calibration and validation data sets solely based on the existing observations, we applied three different approaches commonly used for accuracy estimation and model selection (Kohavi, 1995; Lendasse et al., 2003): 'hold-out', 'leave-one-out' and 'bootstrap':

With the ***hold-out*** (HO) technique the available data set of length $n = 14$ was randomly split into two mutually exclusive subsets. Roughly one third of the data (i.e., a subset of 5 observations) was set apart for validation (i.e., sampled without replacement), while the larger subset containing the remaining two thirds (i.e. 9 observations) of the data was used for calibration (Kohavi, 1995). This procedure was repeated 1000 times to ensure that a wide range of possible combinations was covered. It should be noted that this procedure is similar to the split-sample test commonly used for systematic testing of hydrological model simulations (Klemeš, 1986).

Leave-one-out (LOO) is a cross-validation technique where one observation from the available data set of length $n = 14$ is chosen for validation, again without replacement. The remaining data ($n\text{-}1 = 13$) are used for calibration (Lendasse et al., 2003). This procedure was repeated $n = 14$ times, to make sure that each observation served as a validation set once. According to Efron (1983), LOO gives nearly unbiased error estimates, but typically with rather high variability, especially if the sample size n is small. This procedure is comparable to the traditional case of simulating an ungauged basin based on all available 'donor' catchments, which are used for calibration.

The ***bootstrap*** (BTS) method (Efron, 1979) creates a so-called 'bootstrap sample' by randomly sampling n instances uniformly with replacement from the original data set of length n (Kohavi, 1995). This new bootstrap sample (with the same size n as the original data) forms the calibration data set, while the original data set serves for validation. Due to the random sampling procedure with replacement, some observations may occur multiple times in the bootstrap sample, while others are not included. On average, however, one bootstrap sample has $0.632 \cdot n$ different observations (Kim, 2009; Kohavi, 1995). This procedure was repeated 1000 times to make it comparable to HO. BTS was shown to provide error estimates with low variability, but tends to be overly optimistic due to overfitting (Efron, 1983)

For each of these three approaches, four regression functions (i.e., linear, exponential, power and logarithmic) were fitted to the calibration data set of each signature, but only the one with the highest coefficient of determination r^2 (Nagelkerke, 1991) was chosen for further validation. The performance of the chosen regression model for each streamflow signature was then evaluated on the different validation data sets (HO, LOO and BOOT) using (1) the coefficient of determination r^2 (Nagelkerke, 1991), (2) the index of agreement d (Willmott et al., 1985), and (3) the normalized root-mean-square error *NRMSE*.

4.4. Predicting combined forest and climate change impacts in ungauged basins

We further utilized some of the identified functional relationships to analyze the extent to which the combined effects of physical catchment alterations and climate change on streamflow can be predicted in ungauged basins. Most of the catchment characteristics chosen in this study (Table 1, properties written in italic) were assumed stationary as they were related to topography and geology/soil, which are unlikely to change by the end of this century. The remaining characteristics were related to forest properties, including forest cover and tree species, which are more likely to change in the near future. Given the role of forest ecosystems in the global carbon cycle (Houghton et al., 2009) and the importance of forestry in Sweden (SLU, 2015) and other parts of the world (Kirilenko and Sedjo, 2007), it is particularly important to improve our understanding of how changes in forest cover due to a continued intensification of the forest industry (Helmisaari et al., 2014) and in particular extensions of managed forest land (Rytter et al., 2013) might influence hydrological behavior. Existing case studies in boreal forests suggest that forest clear-cuttings reduce interception and transpiration (Buttle and Metcalfe, 2000), which leads to earlier snowmelt (Schelker et al., 2013), increasing total runoff (Bosch and Hewlett, 1982; Sahin and Hall, 1996), as well as larger peak flows originating from both snowmelt and rainfall events (Guillemette et al., 2005). Global warming and changing precipitation patterns are likely to further amplify some of these effects (Tong et al., 2012), even though the precipitation patterns are more difficult to predict (Kotlarski et al., 2014). It requires sufficiently long data series to analyze and better understand these complex processes within the climate-forest-water nexus. Since the majority of watersheds of the world, however, are ungauged (Sivapalan et al., 2003), our understanding of their behavior under *stationary* climate conditions is inadequate to project *changing* climate conditions with a sufficient level of confidence. This problem is accentuated further when it comes to future projections in ungauged basins that are additionally affected by human activities such as landuse change (Sivapalan, 2003).

Due to a lack of study catchments with actual forest alterations, we created two hypothetical cases of forest disturbance, one representing a forest clear-cut (deforestation) and one representing afforestation in an ungauged basin. We then tried to estimate and compare (1) the consequences of virtual forest disturbances, (2) the influence of climate change, and (3) their combined impact on the hydrological behavior of

a hypothetically ungauged catchment by utilizing the previously identified and validated functional relationships.

4.4.1. Case 1: clear-cut at site C13

In case 1, site C13 was considered an ungauged basin. It had an upstream catchment area of 7 km^2 and was covered by 88% forest, had no open land and 10% wetlands. In a first step, regression models (cf., section 4.3) with forest cover as predictor variable were fitted to all possible streamflow signatures for the reference period ($S_{1981–2010}$) and the projected future changes in streamflow signatures (%ΔS) based on LOO, using only n-1 = 13 'donor' catchments (i.e., leaving out the hypothetically ungauged basin). The calibrated regression equations were then applied to estimate both present-day ($S_{1981–2010}$) and future streamflow signatures ($S_{2061–2090}$) in this particular (hypothetically) ungauged basin based with its original unchanged forest cover of 88%. Consequently, this first step provided an estimate of climate change impacts on streamflow signatures, without considering forest disturbance. These results were validated by comparing them to the originally simulated signatures at C13 (cf., section 4.2).

Thereafter, we assumed a virtual clear-cut reducing the existing forest cover in C13 from 88% to 83%, which equaled an area of 0.35 km^2. This particular reduction was chosen to ensure that the results obtained by the regression analysis could be compared to the originally simulated signatures (cf., section 4.2) of another otherwise similar catchment. Here we compared the regression results to C12 (hereafter referred to as the 'control' catchment), which had similar soil and geological features, but only 83% forest cover (compared to 88% in C13). The regression models calibrated in step 1 with forest cover as independent variable and present-day signatures ($S_{1981-2010}$) as response variables were now used to estimate streamflow signatures during the reference period assuming the above-mentioned reduced forest cover of 83%. Thus, this second step provided an estimate of the consequences of forest disturbance, without considering climate change.

In the final step, the regression models calibrated in step 1 with forest cover as independent variable and the projected future changes in streamflow signatures (%ΔS) as response variables were used to estimate future streamflow signatures ($S_{2061-2090}$) assuming the above-mentioned reduced forest cover of 83%. In other words, this third step considered the combined effects of both climate change and forest disturbance.

4.4.2. Case 2: afforestation at site C10

In case 2, site C10 was chosen to be the hypothetically ungauged basin. This subcatchment with an area of 3.4 km^2 was covered by 74% forest and 26% wetlands. We here created a scenario where roughly one third of the catchment's wetlands was hypothetically drained and then used for afforestation, leading to an increased forest cover of 84% (i.e., 0.34 km^2 more forest). We followed the same procedure as in case 1 to calibrate and utilize the regression models for present and future conditions. The results from the regression analysis were compared to C09 (hereafter referred to as 'control' catchment), which had soil and forest-composition features rather similar to C10, but had a larger area covered by forest (84% compared to 74% in C10).

5. Results

5.1. Changes in climate conditions

Our ensemble of RCM simulations covered a broad range of possible future changes (Fig. 4), which consistently projected an increase in annual temperature, precipitation and potential evapotranspiration. Considering only the ensemble median, the catchment was projected to be 3.7 °C warmer (Fig. 4a), receive 0.3 $mm \cdot d^{-1}$ or 17% more precipitation (Fig. 4b), and be subject to 0.2 $mm \cdot d^{-1}$ or 15% higher annual potential evapotranspiration (Fig. 4c). All three meteorological variables were projected to rise during all seasons, but to a different extent (Fig. 4). Colder seasons such as autumn and winter will likely experience a stronger warming (+3.9 °C respective +4.3 °C), while spring and summer temperatures will increase less strongly by 3.3 °C and 3.1 °C, respectively (Fig. 4a). The expected future warming in the catchment will push the spring thaw three weeks earlier and cause a temporal shift in seasons (not shown here, cf. Teutschbein et al. (2015)), which implies that the period with temperatures below 0 °C is projected to shorten noticeably. Our simulations indicate that this also affects the rain-to-snow ratio: While 66–72% of all precipitation are currently rain, a considerably larger proportion (76–84%) will be rain in the future.

Precipitation projections were somewhat more uncertain, as a few individual RCMs indicate the possibility of no change or even a decrease in precipitation during spring and autumn (Fig. 4b). According to the median, precipitation over the catchment will likely increase about 6% in summer, 17% in autumn and 26% in winter and spring. Potential evapotranspiration showed the largest absolute increase in summer (when potential evapotranspiration is relatively high), and the largest percentage increase in winter (when potential evapotranspiration is typically very low).

5.2. Hydrological modeling

5.2.1. Calibration and validation

For the period 2008–2013 with available streamflow measurements, the HBV model driven with observed temperature and precipitation provided satisfying simulations: With generally high values of R_{eff} (0.7–0.9), L_{eff} (0.6–0.8) and VE values (0.9–1.0), the fuzzy measure X ranged from 0.7 to 0.9, where 1.0 equals a perfect fit. For site C07, the fuzzy measure decreased from 0.8 during the calibration period to 0.7 during the independent validation period, indicating that the agreement between observed and modeled values was generally weaker during the validation. Due to the fact that the validation period was characterized by considerably different meteorological conditions from the calibration period (0.7 °C lower mean temperature, 10% less precipitation), the relatively high value of 0.7 for the fuzzy measure suggested that the model is transferable to conditions different from those corresponding to the calibration record (Klemeš, 1986), although it is not able to capture all climate-driven dynamics.

For a more detailed assessment, a Taylor diagram (Fig. 5) was created to visualize additional evaluation metrics. The Taylor diagram indicated a good model fit with high correlations between observed and simulated streamflow for all 14 catchments. The radial distance from the origin embodies the ratio of standard deviations of the simulated and observed time series. A perfect model with the same standard deviation as the observations (located on the outer circle with a standard deviation equal to one) and a correlation of one would thus fall on point 'OBS'. For all catchments, the correlation between observed and simulated streamflow was within a range of 0.82 and 0.95. The RMSD (normalized by the observed standard deviation) varied from 0.30 to 0.57, and the normalized standard deviation from 0.84 to 1.01. The Taylor diagram also revealed that HBV underestimated the observed streamflow variability in all catchments. Furthermore, HBV performed best for catchment C13, whereas all other catchments were clustered around slightly lower values.

5.2.2. Streamflow simulations in a changing climate

Simulations indicated a clear shift of the hydrological regime in all 14 catchments (Fig. 6). The typical annual flow regimes, which are currently characterized by a large spring flood peak (usually in late April or early May) and noticeably lower streamflow during the rest of the year (Fig. 6a), will in a future climate feature more steady flow conditions (Fig. 6b) as a consequence of increasing winter streamflow in combination with lower and early spring flood peaks (Fig. 6c). Summer flows will experience only minor changes, while the duration

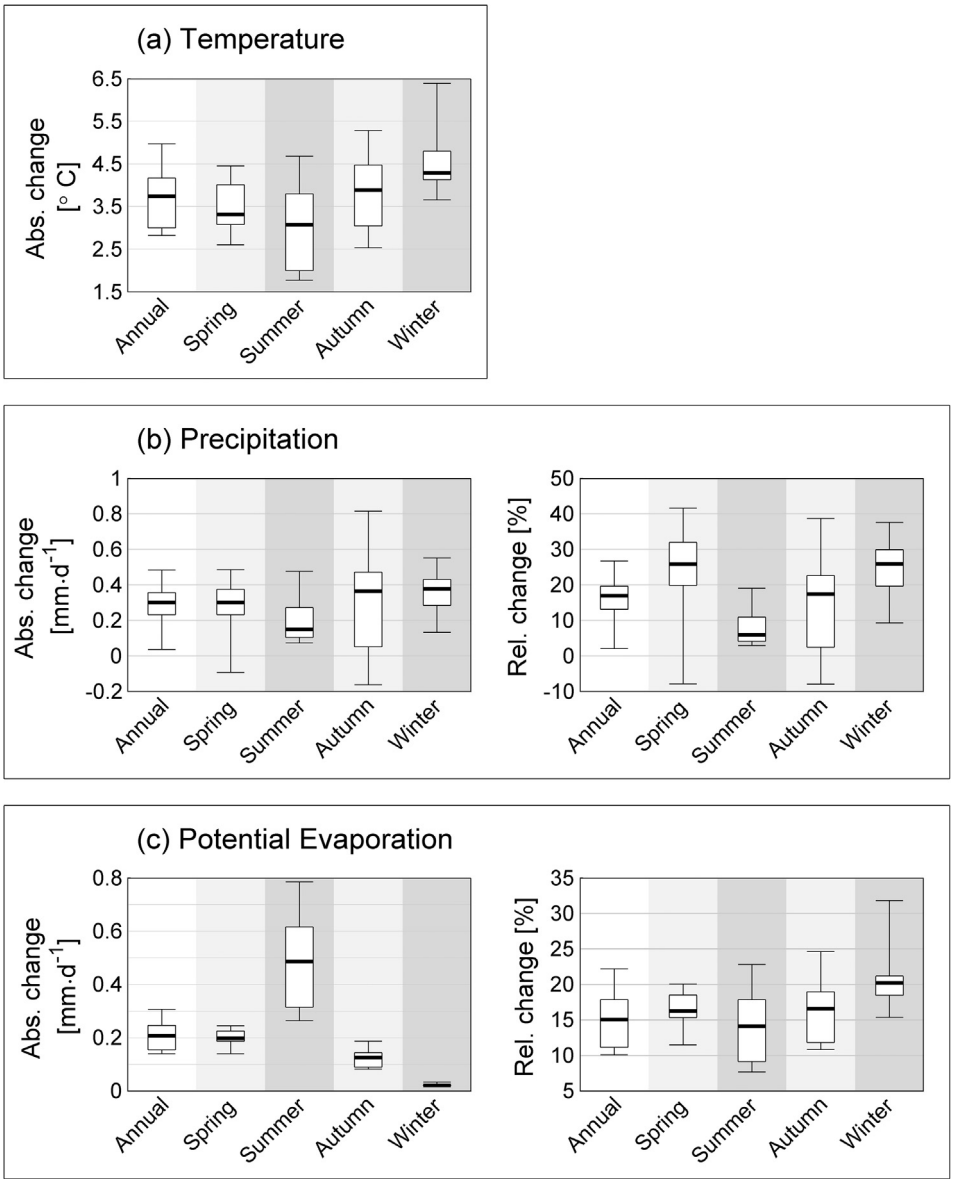

Fig. 4. Projected annual and seasonal meteorological changes in the Krycklan catchment for (a) temperature, (b) precipitation and (c) potential evapotranspiration. Absolute changes are shown on the left, relative changes on the right.

of spring floods will be shorter in a future climate (Fig. 6c).

5.3. Streamflow signature analysis

The selected signatures (Table 3) were computed for (1) HBV-simulated streamflow based on observed meteorology (1981–2010), (2) HBV simulations driven by the RCM-climatology during the reference period 1981–2010 and (3) HBV simulations driven by the RCM-climatology during the future period 2061–2090. The study by Teutschbein et al. (2015), which was based on the same set of catchments and hydrological simulations, already compared the signatures for case one (based on observations) and two (based on RCM-simulations) above. They concluded that RCM-driven HBV simulations were suitable for climate change impact studies, because the majority of RCM-simulated signatures featured biases of less than 10%.

Here, we focused instead on the comparison of the signatures for case two and three above, i.e. future versus present-day regionalized signature responses (Fig. 7). According to our simulations, all annual hydrograph features, i.e., annual mean streamflow ($FMean_{ANN}$), baseflow ($BMean_{ANN}$), and base flow index (BFI_{ANN}) were projected to increase in the future. In terms of seasonal changes, FMean was projected to rise during autumn and winter, but slightly decrease during spring and summer. BMean, on the other hand, featured an increase during all seasons, although the increase was only weak in summer. The seasonal BFI was projected to escalate considerably in spring and only slightly in summer, while the simulations indicated a slight BFI reduction during autumn and winter. All signatures related to the spring flood showed reduced values, i.e., an earlier initiation of the flood, a lower peak, a shorter duration and a smaller volume (Fig. 7). The analysis of signatures related to the flow duration curves indicated reduced high-segment flows, while median and low-segment flows were projected to increase, which indicated a changing tilt of the duration curves. This was also reflected in a slight reduction of the mid-segment slope, a reduced CV and a smaller streamflow skewness (Fig. 7).

In general, most signatures were projected to change in the range of ± 50%. However, a few signatures related to low-flow conditions such as $FMean_{DJF}$, $BMean_{DJF}$, $BMean_{MAM}$, BFI_{MAM} and FLS will likely experience much stronger changes. This can, however, be explained by the fact that the projected changes were given in percentages, which caused a disproportionally large inflation of the apparent deviation at low flows.

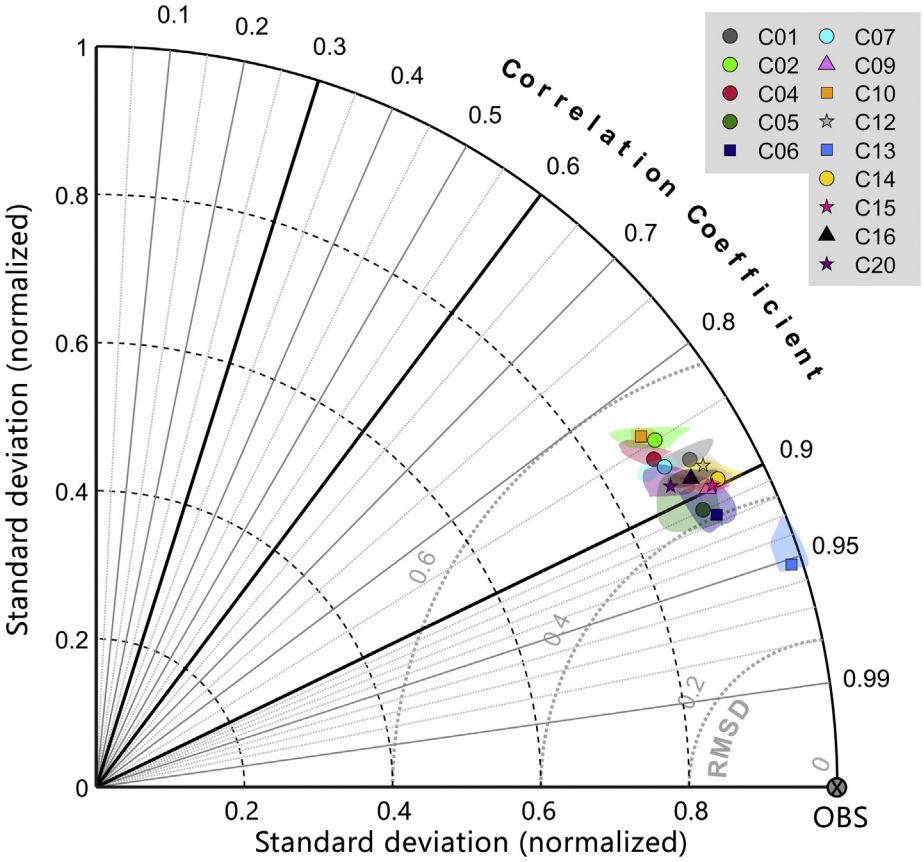

Fig. 5. Taylor diagram for evaluating HBV model performance after calibration for each individual catchment (different color-coding) during the period 2008–2013. The similarity between HBV-simulated and observed streamflow is quantified in terms of their correlation, their centered root-mean-square difference (RMSD) and their standard deviation. Note that if HBV-simulated streamflow would perfectly agree with observed values, the colored circles would fall on point 'OBS'. The colored shaded areas represent the range of streamflow simulations based on the 100 different optimal parameter sets. The colored symbols represent the median of these simulations for each catchment.

5.4. Relationship between landscape characteristics and hydrological change

5.4.1. Identification of correlations and functional relationships

The computed Spearman rank correlation matrix between landscape characteristics and streamflow signatures (Fig. 8a) highlighted a number of significant correlations at the 5% significance level. Of the 286 possible relations between the 11 selected landscape characteristics (Table 1) and 26 streamflow signatures, 65 pairs (23%) were significantly correlated (Fig. 8a). Furthermore, each landscape characteristic was significantly correlated to at least two changes in streamflow signatures. Generally, landscape characteristics such as forest, till, birch and area featured the most frequent and strongest correlations, while pine, aspect and curvature featured the least and weakest correlations. The strongest significant correlations were, however, found between area and low-segment flow FLS ($\rho_s = +0.82$), forest and summer baseflow index BFI_{JJA} ($\rho_s = +0.79$), forest and high-segment flow FHS ($\rho_s = -0.79$), forest and spring flood magnitude ($\rho_s = -0.78$), as well as forest and annual mean streamflow $FMean_{ANN}$ ($\rho_s = +0.77$).

Two-parametric regression functions at the 5% significance level with r^2 values ranging from 0.28 to 0.67 (see Supplemental Information, Table S1) were successfully fitted to 38 out of the 65 significantly correlated pairs, which represented roughly 13% of all possible combinations. Four of these pairs had r^2 values of more than 0.6 (Fig. 8b). Three landscape characteristics (i.e., aspect, curvature and pine) were not useful explanatory variables in two-parametric regression functions. Additionally, we did not succeed to fit two-parametric regression functions for predicting eight of the available streamflow signatures (i.e., summer/winter mean streamflow, annual/summer/winter mean baseflow, autumn baseflow index, total spring flood volume and spring flood duration).

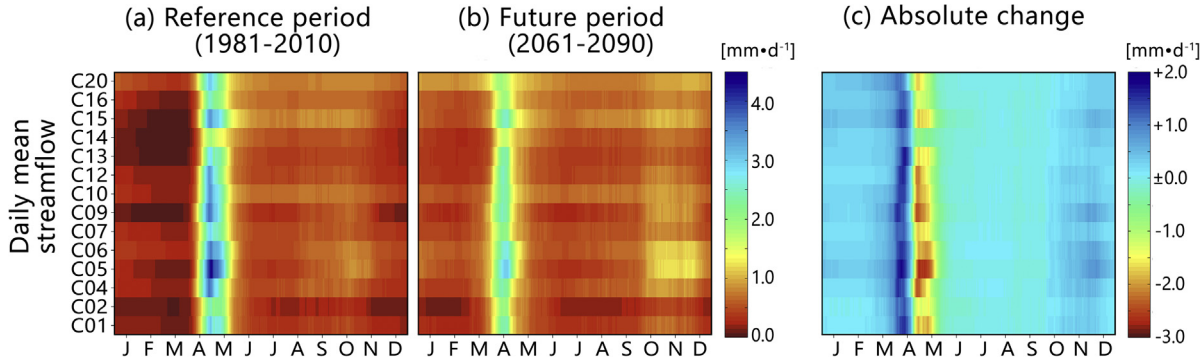

Fig. 6. Comparison of intra-catchment variability of simulated streamflow for the reference period (a), the future period (b) and for the absolute difference between these two periods (c). Higher streamflow values and increasing values are displayed in dark blue, lower streamflow values and projected decreasing values are shown in red (see color bars). (For interpretation of the references to color in this figure legend, the reader is referred to the web version of this article.)

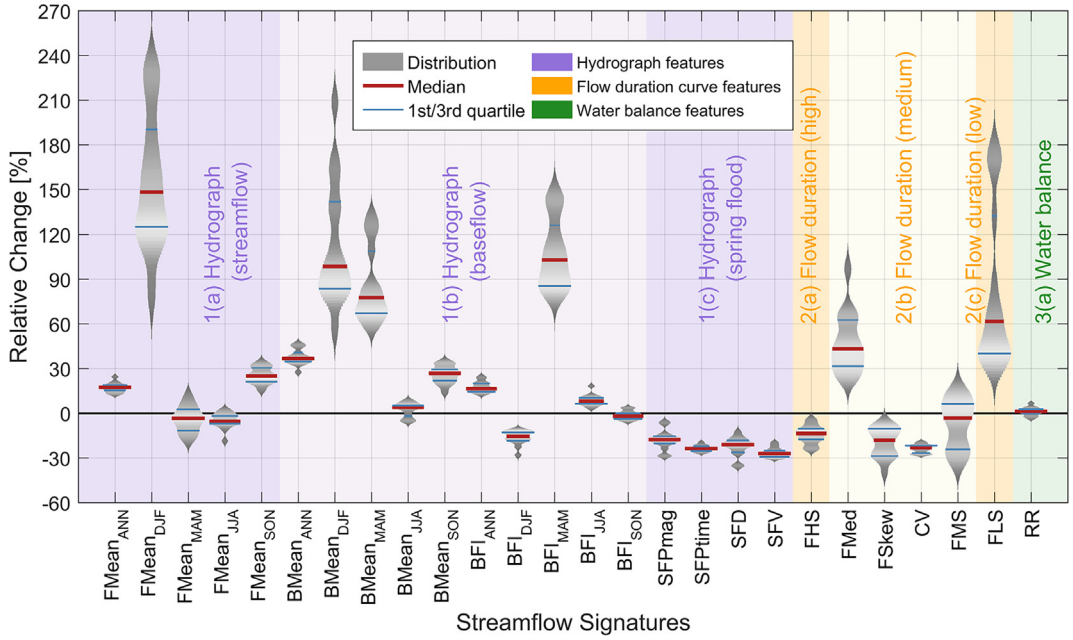

Fig. 7. Projected future changes (in percentage) for signatures related to the hydrograph (purple background), the flow duration curve (yellow background) and the water balance (green background). The gray violin boxes show the inter-catchment variations. The red lines correspond to the median, while blue lines represent the 25th and 75th percentile, respectively. (For interpretation of the references to color in this figure legend, the reader is referred to the web version of this article.)

5.4.2. Validation of functional relationships using Holdout, Leave-one-out and bootstrap method

After having identified 38 significant functional relationships between boreal landscape forms and projected changes in streamflow signatures, we made an attempt to calibrate the regression functions on a subsample of the available data (so-called training set) and to validate the regression model on another set of data. For all three validation approaches employed here (i.e., HO, LOO, BTS), the averaged performance measures indicated a reasonable fit of the regression models for the validation dataset (Fig. 9). We obtained median values ranging from 0.38 (HO) to 0.53 (BTS) for the coefficient of determination (r^2), while the index of agreement was 0.77 for HO, 0.80 for LOO and 0.81 for BTS. The NRMSE had somewhat higher values for HO (i.e., 0.37) and lower values of 0.30 and 0.34 for LOO and BTS, respectively. Summarizing all three performance measures, the best performance was achieved when validating on a bootstrap sample, while the regression models seemed to perform slightly worse when calibrating with help of LOO or HO. In addition, BTS showed the lowest variability based on the interquartile ranges.

5.5. Predicting combined forest and climate change impacts on hydrological behavior of ungauged basins

Only for four streamflow signatures (i.e., $FMean_{ANN}$, SFP_{mag}, FHS and RR), regression functions with forest cover as predictor were significant at the 5% significance level for both the present-day streamflow signatures ($S_{1981–2010}$) and the future percentage change ($\%\Delta S$). The fitted regression models had r^2 values between 0.39 and 0.55. As FHS is highly correlated with SFP_{mag} and almost identical results were obtained, FHS results are not shown separately.

5.5.1. Case 1: clear-cut at site C13

Fig. 10 provides an overview of the fitted regression curves under present and future climate conditions, and shows the simulated signature alterations for the deforestation case. Under present conditions, site C13 with a forest cover of 88% was characterized by an annual mean streamflow ($FMean_{ANN}$) of 283 mm per year, a springflood peak (SFP_{mag}) of 8.3 mm per day, and a runoff ratio (RR) of 0.43 (Fig. 10a–c, blue triangles). Using a regression model to estimate these three values as if C13 were an ungauged basin resulted in deviations between 9 and 13% from the above original values (Fig. 10a–c, blue bars). Both $FMean_{ANN}$ and RR were overestimated each by 13%, while SFP_{mag} was underestimated by 9%.

Considering only the effect of climate change, the regression analysis (Fig. 10a–c, red bars) indicated the same direction of change as the actual values (Fig. 10a–c, red triangles). Both $FMean_{ANN}$ and RR were projected to increase by +18% respective +2%, but were overestimated by the regression function. SFP_{mag} was projected to decrease by 16%, but was at the same time underestimated by roughly 11%.

According to the regression functions, the virtual forest clear-cut would result in a 5% to 6% increase in all three signatures (Fig. 10a–c, green bars) compared to the simulations under present conditions (Fig. 10a–c, blue bars). This was in line with the trend in the actual values of C12 (Fig. 10a–c, green squares), which was used here as control catchment for comparison as it had a natural forest cover of only 83% (the same as C13 after the virtual forest clear-cut).

For the combined influence of forest and climate change (Fig. 10a-c, yellow bars), the direction of change was simulated correctly with the regression models (i.e., an increase in $FMean_{ANN}$ and RR, and a decrease in SFP_{mag}). Given that both climate change and forest clear-cut were projected to elevate $FMean_{ANN}$ and RR, it is not surprising that their combined impact (Fig. 10a and c, yellow bars) boosted both signatures even more. In contrast, SFP_{mag} was projected to decrease as a consequence of climate change (Fig. 10b, red bar), but increase as a consequence of forest clear-cut (Fig. 10b, green bar). This led to a mutual weakening of these external impacts on spring flood peak magnitude.

Regression models fitted the present-day streamflow signatures well (Fig. 10d–f) with r^2 values ranging from 0.41 to 0.54. All three signatures showed a negative relationship with forest cover.

Similarly, regression models for the projected relative change (Fig. 10g–i) showed a good performance with r^2 values between 0.45 and 0.50. However, the relative change in C13 due to climate change was underestimated for all three signatures (Fig. 10g–i, red triangle), while control site C12 was close to the regression line.

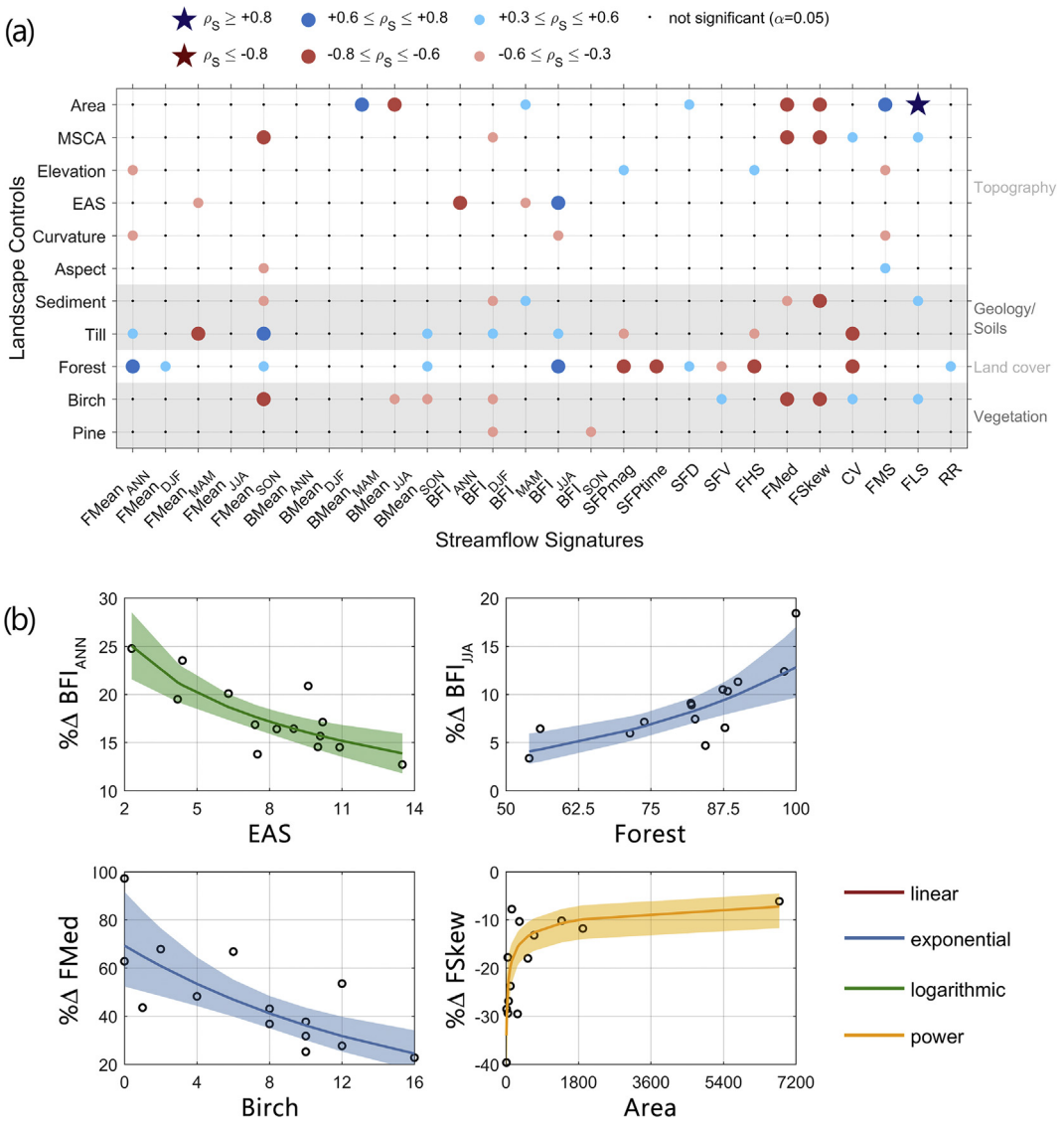

Fig. 8. Relationships between selected landscape controls and projected change in streamflow signatures displayed as (a) Spearman's rank correlation matrix (5% significance level) and (b) scatter plots with fitted two-parametric functions (including 95% confidence intervals around mean response) for pairs with $r^2 > 0.6$.

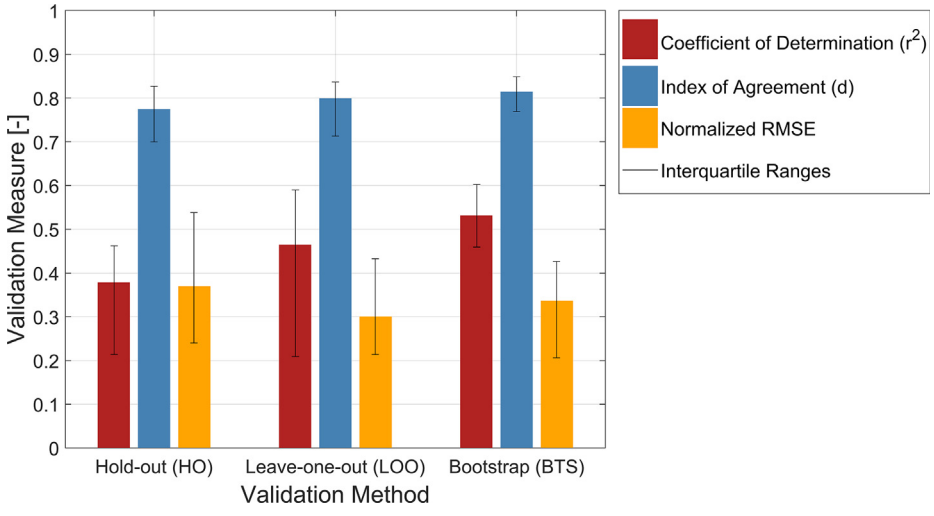

Fig. 9. Overview of average regression model performance using three different methods for validation (i.e., hold-out (HO), leave-one-out (LOO) and bootstrap (BTS)), assessed by three different evaluation criteria, namely the coefficient of determination (r^2), the index of agreement (d) and the normalized root mean squared error (NRMSE).

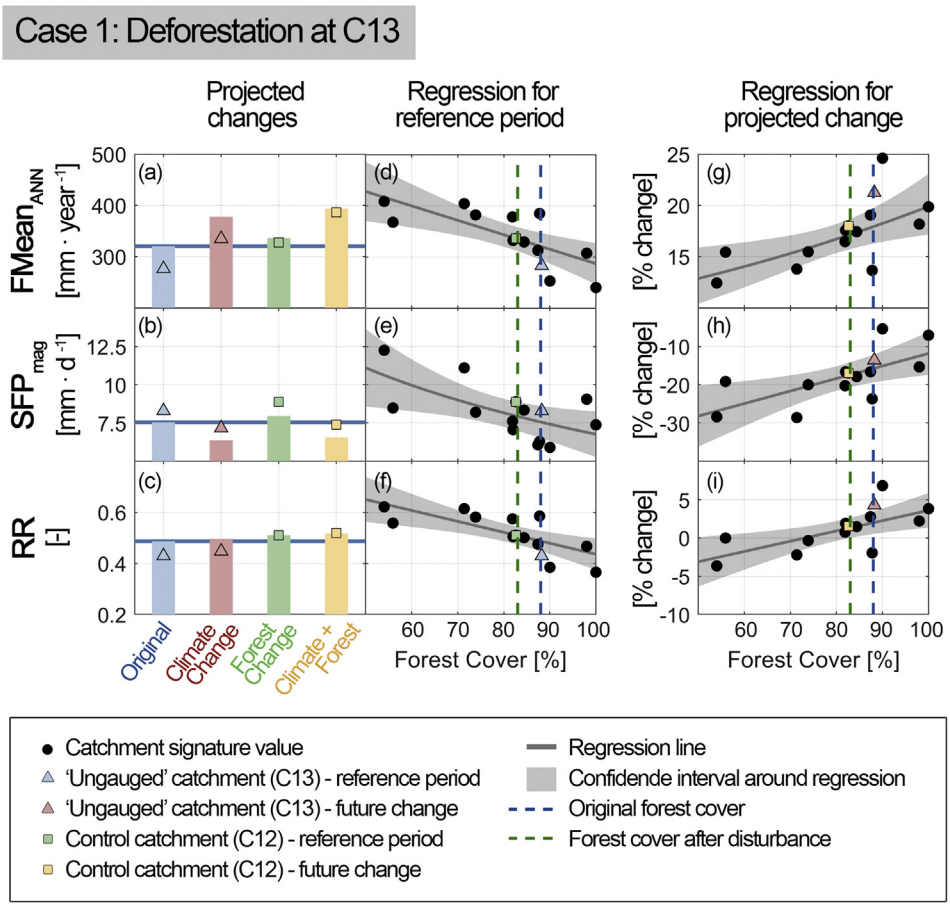

Fig. 10. Simulated impacts of climate change (red), deforestation (green) and a combination of both (yellow) on annual mean streamflow $FMean_{ANN}$ (first row), spring flood peak magnitude SFP_{mag} (second row) and runoff ratio RR (third row) of the hypothetically ungauged basin C13 in case 1. Subplots (a)–(c) show the absolute signatures as simulated by the regression functions (colored bars) in comparison with the original signatures for C13 (triangles) and the control catchment C12 (squares) as derived from the RCM-HBV simulations. Subplots (d)–(f) contain the regressions fitted to the present-day streamflow signatures as derived from the RCM-HBV simulations based on n − 1 = 13 observations without the 'ungauged' basin C13. Subplots (g)–(i) display the regressions fitted to the projected relative change in these streamflow signatures. (For interpretation of the references to color in this figure legend, the reader is referred to the web version of this article.)

5.5.2. Case 2: afforestation at site C10

Fig. 11 summarizes the modeling for the afforestation case. Site C10 with a forest over of 72% had a mean annual streamflow of 382 mm per year under present-day climate conditions. It exhibited a SFPmag of 8.3 mm per day (same as C13) and a RR of 0.58 (Fig. 11a–c, blue triangles). These three values were simulated rather well with a regression model (Fig. 11a–c, blue bars), which deviated only between −7% ($FMean_{ANN}$ and RR) and +7% (SFP_{mag}) from the original value.

In terms of climate change effects, C10 showed a similar pattern as C13 in case 1: Both $FMean_{ANN}$ and RR were projected to increase (+16% respective +0.3%), while SFP_{mag} was projected to decrease by 20% (Fig. 11a–c, red bars).

Modeling results for the afforestation case at site C10 (Fig. 11a–c, green bars) showed the opposite signals compared to the clear-cut in case 1 (Fig. 10a–c, green bars). The virtual afforestation would result in a 8% to 9% decrease in all three signatures (Fig. 11a–c, green bars) compared to the simulations under present conditions (Fig. 11a–c, blue bars). This was in line with the trend in the actual values of control catchment C09 (Fig. 11a–c, green squares).

The regression models showed a very good performance in simulating the combined influence of forest and climate change with deviations of only 1% to 4%. $FMean_{ANN}$ and RR were projected to increase, while SFP_{mag} simulations tended towards a decrease.

The regression curves matched the present-day streamflow signatures well (Fig. 11d–f) with r^2 being in the range of 0.40 to 0.53. Similarly, regression models for the projected relative change (Fig. 11g–i) showed also a good performance (r^2 = 0.45–0.46). This relative change in C10 due to climate change (Fig. 11g–i, red triangle) was better simulated than the change for C13 in case 1 (Fig. 10g–i, red triangle).

In both virtual cases, forest alterations and changing climate conditions considerably affected streamflow signatures (Fig. 10 and Fig. 11). The combined effect of both forest and climate change differed markedly from the individual changes caused solely based on either climate change or forestry impacts. Overall, climate change was the dominant factor driving the changes in $FMean_{ANN}$ and SFP_{mag} in both hypothetical forest alteration cases, while RR was more effected by forest alterations.

Furthermore, a comparison of the regression-based simulations with the original projections for the hypothetical ungauged and the control catchments (cf., section 4.4) revealed that the regression models captured the general signal in the ungauged basins well. In all cases, the direction of change was simulated correctly with deviations between −11% and +13% in the magnitude of change.

6. Discussion

6.1. Changes in climate conditions

Projections based on an ensemble of 15 RCM-GCM combinations under GHG emission scenario A1B provided by the ENSEMBLES project (Van der Linden and Mitchell, 2009) pointed towards increasing precipitation, temperature and potential evapotranspiration for all months of the year until the end of this century, though the projections of precipitation are less certain than those for temperature (Kotlarski et al., 2014). The obtained change signals are comparable to changes summarized by both the ClimateCost project (Christensen et al., 2011) and the Fifth Assessment Report (AR5) of the United Nations Intergovernmental Panel on Climate Change (IPCC, 2014).

The changing climate conditions are expected to have multifold impacts on the environment and will inevitably affect catchment hydrology: higher future precipitation will strongly influence the

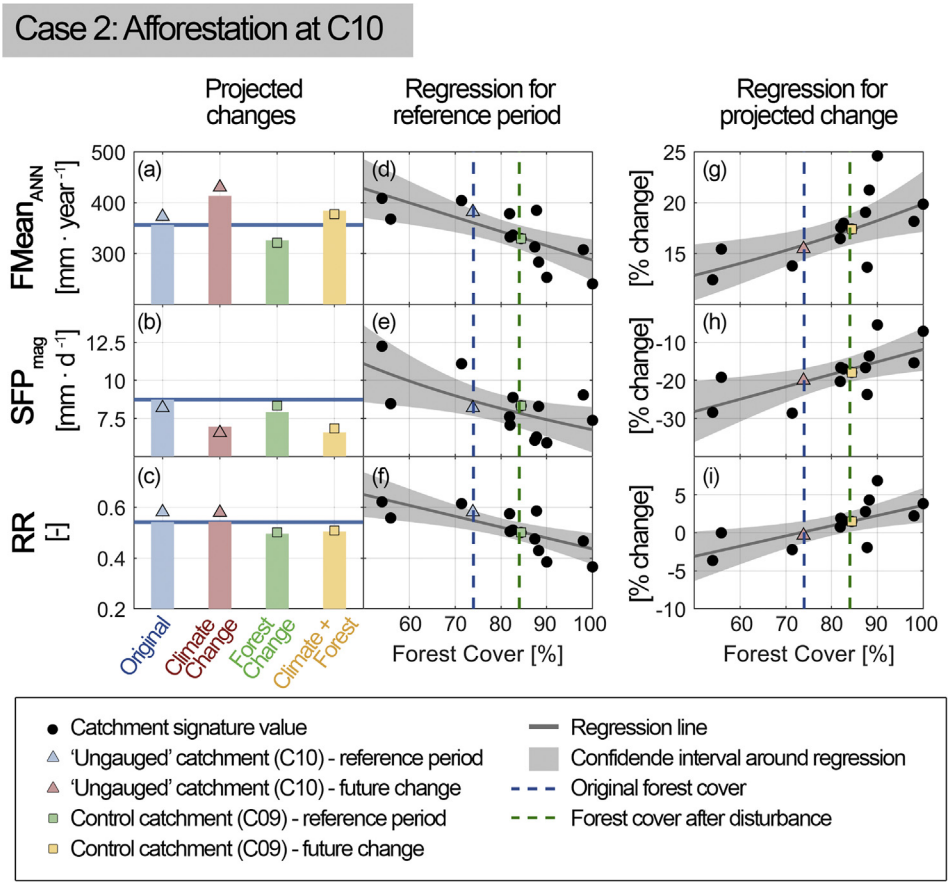

Fig. 11. Simulated impacts of climate change (red), afforestation (green) and a combination of both (yellow) on annual mean streamflow $FMean_{ANN}$ (first row), spring flood peak magnitude SFP_{mag} (second row) and runoff ratio RR (third row) of the hypothetically ungauged basin C10 in case 2. Subplots (a)–(c) show the absolute signatures as simulated by the regression functions (colored bars) in comparison with the original signatures for C10 (triangles) and the control catchment C09 (squares) as derived from the RCM-HBV simulations. Subplots (d)–(f) contain the regressions fitted to the present-day streamflow signatures as derived from the RCM-HBV simulations based on n − 1 = 13 observations without the 'ungauged' basin C10. Subplots (g)–(i) display the regressions fitted to the projected relative change in these streamflow signatures. (For interpretation of the references to color in this figure legend, the reader is referred to the web version of this article.)

catchment's hydrology through changes in spring floods and aquifer recharge. Due to increasing temperatures, spring thaw is expected to occur about 3 weeks earlier, which in turn will have considerable consequences for both snow accumulation, soil frost and water storage in the area. On top of these direct climate change effects on the water balance, changes in precipitation and temperature may also alter the vegetation and local climate feedbacks, and thereby indirectly influence streamflow and hydrological partitioning (Zhang et al., 2018). It is worth noting that the here adopted modeling approach is not able to explicitly account for these alterations (possibly into ranges outside the historical observations which are used for regionalization) and the consequent indirect effects on a catchment's hydrology. In addition, a longer growing season combined with increasing CO_2 levels will affect stomatal conductance and transpiration of trees (Donohue et al., 2017; Trancoso et al., 2017; Yang et al., 2016) and, therefore, have the potential to considerably influence the annual water balance (Gedney et al., 2006; Hasper et al., 2015; Trancoso et al., 2017; Ukkola et al., 2015).

In our study, the projected streamflow changes are conditional on the assumption that the biomass remains constant and that vegetation response will not change considerably. The latter assumption is justified by the fact that the exact vegetation responses to increasing CO_2 levels are still not fully understood (Mengis et al., 2015), which adds an extra layer of uncertainty in hydrological climate change impact studies. However, we found that biomass is indeed an important variable under our static vegetation response assumption, which highlights the importance to better understand vegetation responses to future climate conditions to allow for more reliable projections of combined landuse and climate change effects.

In addition, it should be noted that a rather simple temperature-based pET estimate (Eq. (4)) was used in our study. Shaw and Riha (2011) highlighted that the successful use of temperature-based pET models on historical data is no guarantee for future accuracy under non-stationary climate conditions, because they do not account for future changes in radiation (Wild, 2009), atmospheric humidity (Willett et al., 2008) and wind speed (McVicar et al., 2012). Consequently, temperature-based approaches are overly sensitive to temperature, which could result in unrealistic drying and excessive hydrologic sensitivity.

6.2. Hydrological modeling

Our analysis of current and future hydrological behavior within the Krycklan catchment in Northern Sweden and its associated subcatchments was based on 43'500 streamflow time series each for the reference period 1981–2010 and for the future period 2061–2090 that were simulated with the HBV-light software. Such a large streamflow ensemble provided a wide variety of possible outcomes but also more robust results, because we considered uncertainties in climate model data by employing 15 different RCM-GCM projections and uncertainties in hydrological model parameters by using 100 optimal parameter sets. It should, however, be noted that the modeling procedure employed here does not cover the full range of uncertainties. For example, we did not account for hydrological model structure uncertainty, which could potentially influence future streamflow simulations (Jiang et al., 2007; Jones et al., 2006; Mendoza et al., 2015; Surfleet et al., 2012). Furthermore, error-prone observational data used for calibration can also lead to potentially large uncertainties (Beven and Westerberg, 2011; Beven, 2002). This is particularly true for precipitation, which is highly spatially variable, and for streamflow, which is estimated from logger measurements with associated rating curve uncertainties (Peña-Arancibia et al., 2015; Petersen-Øverleir, 2004; Tomkins, 2014; Westerberg et al., 2016) and gaps when the streams were covered by ice (Karlsen et al., 2016b).

Nonetheless, we were able to demonstrate that the HBV-model is

suitable to effectively simulate hydrological regimes for each individual catchment when driven with observed climate data. Teutschbein et al. (2015) showed that HBV even performs well when driven with RCM-simulated climate data during the reference period 1981–2010, which is essential for drawing meaningful conclusions about potential future streamflow changes.

Our simulations of such future changes in Krycklan and its associated subcatchments were comparable to other recent studies over Sweden (Arheimer and Lindström, 2015; Beldring et al., 2008; Graham et al., 2007a, 2007b; Teutschbein et al., 2011; Teutschbein and Seibert, 2012) and revealed that future streamflow is subject to substantial alterations as a consequence of changes in external climate conditions.

6.3. Streamflow signature analysis

Streamflow signatures were used here to provide a more in-depth picture of the relative changes in individual hydrological components of the overall water balance, the hydrograph and flow duration curves, which may not have been apparent from the response time series alone (Yilmaz et al., 2008).

Our comparison of regionalized response signatures for present and future climate conditions highlighted a couple of clear hydrological alterations caused by a changing climate: the present streamflow regimes with large snowmelt-driven spring floods and rather low winter baseflows can be expected to change to regimes with a much earlier onset of spring flood and less extreme flows (both high and low). Arora and Boer (2001) argued that such marked hydrological changes typically reflect alterations in a catchment's input, storage or release of water. The input (i.e., precipitation) was projected to increase throughout all seasons, which explains the higher annual mean streamflow. Although even mean baseflow was projected to increase, the future BFI was projected to decrease. These latter projections, however, should be interpreted with caution. Baseflow is usually regulated by groundwater, surface water, snow, and ice-related processes (Beck et al., 2013b). In our study, however, baseflow was separated with a simply recursive digital filter, which removes high-frequency signals without any physical basis (Nathan and McMahon, 1990; Ladson et al., 2013; Chapman, 1991). Consequently, the projected changes in baseflow and BFI do not allow any conclusions concerning possible shifts in storm-driven rapid flows. But the decreasing BFI can be seen as an indication for more high-frequency rain-driven signals in the future streamflow simulations, especially during winter as a consequence of an overall increase in precipitation and a shift from snow- to rain-dominated precipitation (Arheimer and Lindström, 2015). This transition in the coming decades will reduce snow accumulation, directly affect the storage capacity and disturb the spatiotemporal distribution of catchment water (Williams et al., 2009). In fact, changes in the rain-to-snow ratio will likely result in a more even distribution of streamflow (i.e., release of water) over time with less streamflow variability as demonstrated in this work. Consequently, future hydrological behavior in boreal Sweden will likely take after today's streamflow regimes of regions much further south with serious consequences for stream connectivity and habitat (Lake, 2003), for stream velocity and sedimentation rates (Wood and Armitage, 1997), and for water quality (Teutschbein et al., 2016).

Our comparison of simulated streamflow signature changes among different catchments revealed clear spatial differences in the magnitude of change, although the general direction of change (i.e., increase or decrease of a signature) was similar for all catchments. This highlights the importance of noting that nearby catchments with seemingly similar landscape forms will not necessarily react in the same way to the same external climate change signal (Teutschbein et al., 2015).

6.4. Landscape characteristics and hydrological change

We were able to identify a large number of significant correlations and functional relationships between landscape forms and projected hydrological change. All but two landscape characteristics showed significant functional relationships to one or more streamflow signature changes. This strongly suggests that land cover, vegetation, soil type and topographic characteristics control the magnitude of climate-change induced catchment-specific streamflow changes. By nature, the here investigated boreal catchments are dominated by forests and wetlands, and have only small fractions of agriculture, open land and lakes (Laudon et al., 2013). Consequently, significant and reliable correlations were found mostly for forest-related (e.g., forest cover or biomass) and wetland-related landscape characteristics (e.g. wetland area or peat soils). An earlier study of the Krycklan catchment already demonstrated that spring flood peak magnitude and timing in wetland-dominated catchments are more sensitive to changing climate conditions than in forested catchments, while annual streamflow and summer base flow are less sensitive (Teutschbein et al., 2015). On the contrary, in forested catchments with little or no wetlands, annual streamflow and summer base flow are more sensitive to changing climate conditions, while the effects on spring flood events are less severe. This can be explained by shallow groundwater tables and transmissivity feedback mechanisms in northern Swedish forests and till soils (Bishop, 1991), which generally cause more flashy hydrologic responses with little storage buffer capacity in drier seasons (Karlsen et al., 2016a). These features affect the hydrological sensitivity of forested areas to changing climate conditions, implying that these results might only be valid for high-latitude catchments in the boreal region. In addition, we believe that this relationship to landscape characteristics might also be a manifestation of the detected change in rain/snow partitioning, i.e., the change in the rain-to-snow ratio affects different landscape forms differently (e.g., different interception rates and albedo control snow accumulation and melt). It should also be noted that summer streamflow may be particularly sensitive to climate-change driven forest changes such as shifting tree species composition, age classes or leaf area (Jones, 2011; Jones et al., 2012) and increasing evapotranspiration due to extended growing season (Huntington et al., 2009). However, understanding these forest responses to changing climate conditions and their impact on the hydrological cycle remains still a major challenge.

Our analysis continued with an attempt to validate the fitted functional relationships (i.e., regression models) on an independent data set by applying three different techniques: 'hold-out' (HO), 'leave-one-out' (LOO) and 'bootstrap' (BTS). Kim (2009) demonstrated that BTS generally works well for small samples. Using BTS in our study resulted indeed in the best overall performance and lowest variability, followed by LOO. It should however be noted that BTS tends to provide biased estimates of the true performance error variance (Braga-Neto and Dougherty, 2004). The resulting values for the coefficient of determination and the index of agreement were promising and suggested that functional relationships between landscape characteristics and projected future streamflow changes could potentially be used to obtain information about the change in an ungauged nearby catchment with known physical catchments characteristics.

6.5. Predicting combined forest and climate change impacts on hydrological behavior of ungauged basins

Numerous studies have shown that both climate and land use change have considerable influence on future streamflow shifts (Bronstert et al., 2002; DeFries and Eshleman, 2004; Mao and Cherkauer, 2009; Oni et al., 2015; Zhang and Schilling, 2006). Bronstert et al. (2002) states that vegetation changes such as forest cutting or afforestation largely affect surface and near-surface hydrological processes such as interception, litter and root zone storage, which are all relevant for evapotranspiration, energy balance and storm runoff generation. But the potential impacts of deforestation or afforestation on streamflow remain contested (Ellison et al., 2012).

Although many studies suggest that deforestation causes annual streamflow to increase while afforestation causes a decrease, there have been some inconsistent responses (Beck et al., 2013a; Lacombe et al., 2016), indicating that dominant eco-hydrological processes and their drivers are highly variable across spatial scales (Zhang et al., 2017).

The two virtual forest experiments designed in our study reinforced the importance of forest cover for hydrological behavior: The amount of forested area in a catchment seems to play a key role in how sensitive different components of a catchment's hydrological regime are to changing climate conditions. This new knowledge is crucial to help forest and water managers understand and predict how forest water quantity and quality is affected across space and over time (The National Academy of Sciences, 2008). For example, Teutschbein et al. (2016) highlighted that rising winter streamflow caused by climate change directly increases the annual inorganic nitrogen loads to the Baltic Sea and accelerates freshwater and marine eutrophication. Considering now the influence of forest cover on different components of the hydrological regime, land cover alterations such as de- or afforestation may amplify or attenuate the effects of climate change on nitrogen loads. Considering these potential challenges and possibilities that come with forest cover alterations, there is a need to develop a framework for conservation and management of forests, which takes into account the implications of a changing climate (Milad et al., 2013). Such a framework could also provide the basis for improving the protection and restoration of stream water quality (Pinay et al., 2015).

It should, however, be noted that the reliability of these kinds of projections depends on the data quality and uncertainties of the gauged catchments as well as on uncertainties in the regionalization approach (Westerberg et al., 2016). By using a regionalization approach, changes in hydrological signatures as a consequence of combined landuse and climate change could generally be predicted for ungauged catchments, especially when evaluating the overall trend of change (i.e., increase or decrease). The magnitude of change, however, showed some deviations, which we believe might have been a consequence of working with too small a number of partly nested gauged basins, with incomplete and partly overlapping landscape characteristics. More advanced methods such as multi-linear regression (Merz and Blöschl, 2004; Ochoa-Tocachi et al., 2016) or copula-based methods (Samaniego et al., 2010) might perform better at predicting the consequences of combined landuse and climate change as such methods are able to account for the interdependence between different landscape characteristics. Furthermore, HBV is a model that does not assimilate land-use information directly, but conceptually translates this information to its parameters. Given the limitations of such conceptual lumped models, using more complex distributed hydrological models might strengthen the analysis of land-use change. To better provide policy-relevant advice to the forestry sector, multi-scale modeling approaches (van Dijk et al., 2007) should be considered. The lumped approach presented herein may not be sufficient to provide accurate information as to where in a catchment to perform clear-cuts or reforestation. To additionally maximize the variability range, one could make a statistically smart choice of a small number of gauged ('donor') catchments, assuming a larger number of gauged catchments is available to choose from (Beck et al., 2016). Ideally, a larger number of gauged basins covering a wider range of percentages of different land covers should be included (Kite and Kouwen, 1992) to feed the regression model calibration with more information and, consequently, to provide more reliable simulations for the ungauged basin. This emphasizes the need for sufficient data from various catchments with a wide variety of boreal landscape forms to increase the information content for calibration and reduce uncertainties in future projections.

7. Conclusion

Different landscape characteristics such as topography, geology, soils and land cover are known to control hydrological behavior of catchments under the same (stationary) climate conditions. Their complex interactions and their combined influence on streamflow are, however, not well understood, especially in the context of climate shifts. Based on the analysis of a *meso*-scale catchment and its associated partly nested subcatchments in Northern Sweden, we demonstrated that landscape characteristics are not only important under *stationary* climate conditions, but also play a fundamental role for the sensitivity of a catchment to *changing* climate conditions. We showed that a regionalization approach can be applied to establish significant functional relationships between different landscape forms and hydrological shifts in a changing climate, which in turn can be used to predict the combined effects of changes in physical catchment and climate conditions on hydrological processes in an ungauged basin. We believe that this approach is versatile and can also be applied to areas with different climate, land use or catchment conditions in other parts of the world. Simulations of two different virtual cases of forest disturbances highlighted the importance of forest cover for the sensitivity of a catchment's hydrological response to changing climate conditions. Further research is still necessary to increase our understanding of how other landscape forms contribute to future streamflow changes, which is key to quantifying the combined impacts of landuse and climate change on storage and release of water as well as on nutrient cycling. Although our findings are limited to a relatively small geographic region and remain to be confirmed for other catchments, we recommend refining present forestry goals and practices given the risks and uncertainties of a changing climate. A framework for conservation and management of forests is needed to promote sustainable forestry that protects forest water quality and ecological flows.

Acknowledgements

The Uppsala University Department of Earth Sciences, Program for Air, Water and Landscape Sciences has funded the lead author. This study is part of the Krycklan catchment study (http://www.slu.se/krycklan), supported by VR, FORMAS (ForWater), Mistra (Future Forests), SKB, and the Kempe Foundation. We especially thank those involved in field work. The ENSEMBLES data used in this work (http://ensemblesrt3.dmi.dk/) were funded by the EU FP6 Integrated Project ENSEMBLES (contract 505539) whose support is gratefully acknowledged. A special thank you to the anonymous reviewers and the editorial team for their highly constructive comments.

Appendix A. Supplementary data

Supplementary data associated with this article can be found, in the online version, at http://dx.doi.org/10.1016/j.jhydrol.2018.03.060.

References

Alexander, L.V., Zhang, X., Peterson, T.C., Caesar, J., Gleason, B., Klein Tank, A.M.G., Haylock, M., Collins, D., Trewin, B., Rahimzadeh, F., Tagipour, A., Rupa Kumar, K., Revadekar, J., Griffiths, G., Vincent, L., Stephenson, D.B., Burn, J., Aguilar, E., Brunet, M., Taylor, M., New, M., Zhai, P., Rusticucci, M., Vazquez-Aguirre, J.L., 2006. Global observed changes in daily climate extremes of temperature and precipitation. J. Geophys. Res.-Atmos. 111, D05109. http://dx.doi.org/10.1029/2005JD006290.

Andréasson, J., Bergström, S., Carlsson, B., Graham, L.P., Lindström, G., 2004. Hydrological change: climate change impact simulations for Sweden. AMBIO 33, 228–234. http://dx.doi.org/10.1579/0044-7447-33.4.228.

Arheimer, B., Lindström, G., 2015. Climate impact on floods: changes in high flows in Sweden in the past and the future (1911–2100). Hydrol. Earth Syst. Sci. 19, 771–784. http://dx.doi.org/10.5194/hess-19-771-2015.

Arora, V.K., Boer, G.J., 2001. Effects of simulated climate change on the hydrology of major river basins. J. Geophys. Res.-Atmos. 106, 3335–3348. http://dx.doi.org/10.1029/2000JD900620.

Beck, H.E., Bruijnzeel, L.A., van Dijk, A.I.J.M., McVicar, T.R., Scatena, F.N., Schellekens, J., 2013a. The impact of forest regeneration on streamflow in 12 mesoscale humid tropical catchments. Hydrol. Earth Syst. Sci. 17, 2613–2635. http://dx.doi.org/10.5194/hess-17-2613-2013.

Beck, H.E., van Dijk, A.I.J.M., de Roo, A., Miralles, D.G., McVicar, T.R., Schellekens, J., Bruijnzeel, L.A., 2016. Global-scale regionalization of hydrologic model parameters: Global-scale regionalization. Water Resour. Res. 52, 3599–3622. http://dx.doi.org/

10.1002/2015WR018247.
Beck, H.E., van Dijk, A.I.J.M., Miralles, D.G., de Jeu, R.A.M., Sampurno Bruijnzeel, L.A., McVicar, T.R., Schellekens, J., 2013b. Global patterns in base flow index and recession based on streamflow observations from 3394 catchments: global patterns in base flow characteristics. Water Resour. Res. 49, 7843–7863. http://dx.doi.org/10.1002/2013WR013918.
Beldring, S., Engen-Skaugen, T., Førland, E.J., Roald, L.A., 2008. Climate change impacts on hydrological processes in Norway based on two methods for transferring regional climate model results to meteorological station sites. Tellus A 60, 439–450. http://dx.doi.org/10.1111/j.1600-0870.2008.00306.x.
Bergström, S., 1992. The HBV Model – Its Structure and Applications, Hydrologi Report RH 4. Swedish Meteorological and Hydrological Institute (SMHI), Norrköping, Sweden.
Bergström, S., 1976. Development and application of a conceptual runoff model for Scandinavian catchments, Report RHO7. Swedish Meteorological and Hydrological Institute (SMHI), Norrköping, Sweden.
Bergström, S., Carlsson, B., Gardelin, M., Lindström, G., Pettersson, A., Rummukainen, M., 2001. Climate change impacts on runoff in Sweden – assessments by global climate models, dynamical downscaling and hydrological modelling. Clim. Res. 16, 101–112. http://dx.doi.org/10.3354/cr016101.
Bergström, S., Lindström, G., 2015. Interpretation of runoff processes in hydrological modelling – experience from the HBV approach. Hydrol. Process. 29, 3535–3545. http://dx.doi.org/10.1002/hyp.10510.
Beven, K., Westerberg, I., 2011. On red herrings and real herrings: disinformation and information in hydrological inference. Hydrol. Process. 25, 1676–1680. http://dx.doi.org/10.1002/hyp.7963.
Beven, K.J., 2002. Rainfall – Runoff Modelling: The Primer, 1st ed. John Wiley & Sons, Chinchester, England.
Bishop, K.H., 1991. Episodic Increases in Stream Acidity, Catchment Flow Pathways and Hydrograph Separation. University of Cambridge, Cambridge, UK Thesis.
Boe, J., Terray, L., Habets, F., Martin, E., 2007. Statistical and dynamical downscaling of the Seine basin climate for hydro-meteorological studies. Int. J. Climatol. 27, 1643–1655. http://dx.doi.org/10.1002/joc.1602.
Bosch, J.M., Hewlett, J.D., 1982. A review of catchment experiments to determine the effect of vegetation changes on water yield and evapotranspiration. J. Hydrol. 55, 3–23. http://dx.doi.org/10.1016/0022-1694(82)90117-2.
Braga-Neto, U.M., Dougherty, E.R., 2004. Is cross-validation valid for small-sample microarray classification? Bioinformatics 20, 374–380. http://dx.doi.org/10.1093/bioinformatics/btg419.
Bronstert, A., Niehoff, D., Bürger, G., 2002. Effects of climate and land-use change on storm runoff generation: present knowledge and modelling capabilities: effects of climate and land-use change on storm runoff generation. Hydrol. Process. 16, 509–529. http://dx.doi.org/10.1002/hyp.326.
Brown, A.E., Zhang, L., McMahon, T.A., Western, A.W., Vertessy, R.A., 2005. A review of paired catchment studies for determining changes in water yield resulting from alterations in vegetation. Journal of Hydrology 310, 28–61. http://dx.doi.org/10.1016/j.jhydrol.2004.12.010.
Buttle, J.M., 1998. Fundamentals of small catchment hydrology. In: Kendall, C., McDonnell, J.J. (Eds.), Isotope Tracers in Catchment Hydrology. Elsevier, Amsterdam, pp. 1–43.
Buttle, J.M., Eimers, M.C., 2009. Scaling and physiographic controls on streamflow behaviour on the Precambrian Shield, south-central Ontario. J. Hydrol. 374, 360–372. http://dx.doi.org/10.1016/j.jhydrol.2009.06.036.
Buttle, J.M., Metcalfe, R.A., 2000. Boreal forest disturbance and streamflow response, northeastern Ontario. Can. J. Fish. Aquat. Sci. 57, 5–18. http://dx.doi.org/10.1139/f00-107.
Carey, S.K., Tetzlaff, D., Seibert, J., Soulsby, C., Buttle, J., Laudon, H., McDonnell, J., McGuire, K., Caissie, D., Shanley, J., Kennedy, M., Devito, K., Pomeroy, J.W., 2010. Inter-comparison of hydro-climatic regimes across northern catchments: synchronicity, resistance and resilience. Hydrol. Process. 24, 3591–3602. http://dx.doi.org/10.1002/hyp.7880.
Chang, H., Jung, I.-W., 2010. Spatial and temporal changes in runoff caused by climate change in a complex large river basin in Oregon. J. Hydrol. 388, 186–207. http://dx.doi.org/10.1016/j.jhydrol.2010.04.040.
Chapman, T.G., 1991. Comment on "Evaluation of automated techniques for base flow and recession analyses" by R. J. Nathan and T A. McMahon. Water Resour Res 27, 1783–1784. http://dx.doi.org/10.1029/91WR01007.
Christensen, O.B., Goodess, C.M., Harris, I., Watkiss, P., 2011. European and Global Climate Change Projections: Discussion of Climate Change Model Outputs, Scenarios and Uncertainty in the EC RTD ClimateCost Project, in: Watkiss, P. (Ed.), The ClimateCost Project. Final Report. Volume 1: Europe. Published by the Stockholm Environment Institute, Sweden, pp. 1–36.
Clausen, B., Biggs, B.J.F., 2000. Flow variables for ecological studies in temperate streams: groupings based on covariance. J. Hydrol. 237, 184–197. http://dx.doi.org/10.1016/S0022-1694(00)00306-1.
Conrad, O., Bechtel, B., Bock, M., Dietrich, H., Fischer, E., Gerlitz, L., Wehberg, J., Wichmann, V., Böhner, J., 2015. System for automated geoscientific analyses (SAGA) v. 2.1.4. Geosci. Model Dev. 8, 1991–2007. http://dx.doi.org/10.5194/gmd-8-1991-2015.
Correa, A., Windhorst, D., Crespo, P., Célleri, R., Feyen, J., Breuer, L., 2016. Continuous *versus* event-based sampling: how many samples are required for deriving general hydrological understanding on Ecuador's páramo region?: Comparison of Continuous *Versus* Event-Based Sampling. Hydrol. Processes 30, 4059–4073. http://dx.doi.org/10.1002/hyp.10975.
DeFries, R., Eshleman, K.N., 2004. Land-use change and hydrologic processes: a major focus for the future. Hydrol. Process. 18, 2183–2186. http://dx.doi.org/10.1002/hyp.5584.
Déqué, M., Rowell, D.P., Lüthi, D., Giorgi, F., Christensen, J.H., Rockel, B., Jacob, D., Kjellström, E., De Castro, M., van den Hurk, B., 2007. An intercomparison of regional climate simulations for Europe: assessing uncertainties in model projections. Clim. Change 81, 53–70. http://dx.doi.org/10.1007/s10584-006-9228-x.
Donohue, R.J., Roderick, M.L., McVicar, T.R., Yang, Y., 2017. A simple hypothesis of how leaf and canopy-level transpiration and assimilation respond to elevated CO2 reveals distinct response patterns between disturbed and undisturbed vegetation. J. Geophys. Res.-Biogeo 122, 168–184. http://dx.doi.org/10.1002/2016JG003505.
Dunne, T., 1978. Field studies of hillslope flow processes. In: Kirkby, M.J. (Ed.), Hillslope Hydrology. John Wiley & Sons, Chichester, pp. 227–293.
Efron, B., 1983. Estimating the error rate of a prediction rule: improvement on cross-validation. J. Am. Stat. Assoc. 78, 316. http://dx.doi.org/10.2307/2288636.
Efron, B., 1979. Computers and the theory of statistics: thinking the unthinkable. SIAM Rev. 21, 460–480. http://dx.doi.org/10.1137/1021092.
Ehret, U., Zehe, E., Wulfmeyer, V., Warrach-Sagi, K., Liebert, J., 2012. HESS Opinions "Should we apply bias correction to global and regional climate model data?". Hydrol. Earth Syst. Sci. 16, 3391–3404. http://dx.doi.org/10.5194/hess-16-3391-2012.
Ellison, D., Futter, M.N., Bishop, K., 2012. On the forest cover-water yield debate: from demand- to supply-side thinking. Global Change Biol. 18, 806–820. http://dx.doi.org/10.1111/j.1365-2486.2011.02589.x.
Farmer, D., Sivapalan, M., Jothityangkoon, C., 2003. Climate, soil, and vegetation controls upon the variability of water balance in temperate and semiarid landscapes: downward approach to water balance analysis. Water Resour. Res. 39, 1035. http://dx.doi.org/10.1029/2001WR000328.
Frisbee, M.D., Phillips, F.M., Weissmann, G.S., Brooks, P.D., Wilson, J.L., Campbell, A.R., Liu, F., 2012. Unraveling the mysteries of the large watershed black box: implications for the streamflow response to climate and landscape perturbations. Geophys. Res. Lett. 39, L01404. http://dx.doi.org/10.1029/2011GL050416.
Gedney, N., Cox, P.M., Betts, R.A., Boucher, O., Huntingford, C., Stott, P.A., 2006. Detection of a direct carbon dioxide effect in continental river runoff records. Nature 439, 835–838. http://dx.doi.org/10.1038/nature04504.
Graham, L., Andréasson, J., Carlsson, B., 2007a. Assessing climate change impacts on hydrology from an ensemble of regional climate models, model scales and linking methods – a case study on the Lule River basin. Clim. Change 81, 293–307. http://dx.doi.org/10.1007/s10584-006-9215-2.
Graham, L., Hagemann, S., Jaun, S., Beniston, M., 2007b. On interpreting hydrological change from regional climate models. Clim. Change 81, 97–122. http://dx.doi.org/10.1007/s10584-006-9217-0.
Graham, L.P., 2004. Climate change effects on river flow to the Baltic Sea. AMBIO 33, 235–241. http://dx.doi.org/10.1579/0044-7447-33.4.235.
Guillemette, F., Plamondon, A.P., Prévost, M., Lévesque, D., 2005. Rainfall generated stormflow response to clearcutting a boreal forest: peak flow comparison with 50 world-wide basin studies. J. Hydrol. 302, 137–153. http://dx.doi.org/10.1016/j.jhydrol.2004.06.043.
Gupta, H.V., Wagener, T., Liu, Y., 2008. Reconciling theory with observations: elements of a diagnostic approach to model evaluation. Hydrol. Process. 22, 3802–3813. http://dx.doi.org/10.1002/hyp.6989.
Harlin, J., Kung, C., 1992. Parameter uncertainty and simulation of design floods in Sweden. J. Hydrol. 137, 209–230. http://dx.doi.org/10.1016/0022-1694(92)90057-3.
Hasper, T.B., Wallin, G., Lamba, S., Hall, M., Jaramillo, F., Laudon, H., Linder, S., Medhurst, J.L., Räntfors, M., Sigurdsson, B.D., Uddling, J., 2015. Water use by Swedish boreal forests in a changing climate. Funct. Ecol. http://dx.doi.org/10.1111/1365-2435.12546. n/a–n/a.
Helmisaari, H.-S., Kaarakka, L., Olsson, B.A., 2014. Increased utilization of different tree parts for energy purposes in the Nordic countries. Scand. J. Forest. Res. 29, 312–322. http://dx.doi.org/10.1080/02827581.2014.926097.
Hirabayashi, Y., Mahendran, R., Koirala, S., Konoshima, L., Yamazaki, D., Watanabe, S., Kim, H., Kanae, S., 2013. Global flood risk under climate change. Nat. Clim. Change 3, 816–821. http://dx.doi.org/10.1038/nclimate1911.
Houghton, R.A., Hall, F., Goetz, S.J., 2009. Importance of biomass in the global carbon cycle. J. Geophys. Res.-Biogeo 114. http://dx.doi.org/10.1029/2009JG000935.
Huntington, T.G., Richardson, A.D., McGuire, K.J., Hayhoe, K., 2009. Climate and hydrological changes in the northeastern United States: recent trends and implications for forested and aquatic ecosystems. Can. J. Forest Res. 39, 199–212. http://dx.doi.org/10.1139/X08-116.
Ines, A.V.M., Hansen, J.W., 2006. Bias correction of daily GCM rainfall for crop simulation studies. Agr. Forest. Meteorol. 138, 44–53. http://dx.doi.org/10.1016/j.agrformet.2006.03.009.
IPCC, 2014. Climate Change 2013: The Physical Science Basis, Contribution of Working Group I to the Fifth Assessment Report of the Intergovernmental Panel on Climate Change. Cambridge University Press, Cambridge, UK, and New York, USA.
Jiang, T., Chen, Y.D., Xu, C., Chen, X., Chen, X., Singh, V.P., 2007. Comparison of hydrological impacts of climate change simulated by six hydrological models in the Dongjiang Basin, South China. J. Hydrol. 336, 316–333. http://dx.doi.org/10.1016/j.jhydrol.2007.01.010.
Jones, J.A., 2011. Hydrologic responses to climate change: considering geographic context and alternative hypotheses. Hydrol. Process. 25, 1996–2000. http://dx.doi.org/10.1002/hyp.8004.
Jones, J.A., Creed, I.F., Hatcher, K.L., Warren, R.J., Adams, M.B., Benson, M.H., Boose, E., Brown, W.A., Campbell, J.L., Covich, A., et al., 2012. Ecosystem processes and human influences regulate streamflow response to climate change at long-term ecological research sites. BioScience 62, 390–404. http://dx.doi.org/10.1525/bio.2012.62.4.10.
Jones, R.N., Chiew, F.H.S., Boughton, W.C., Zhang, L., 2006. Estimating the sensitivity of

mean annual runoff to climate change using selected hydrological models. Adv. Water Res. 29, 1419–1429. http://dx.doi.org/10.1016/j.advwatres.2005.11.001.
Karlsen, R.H., Grabs, T., Bishop, K., Buffam, I., Laudon, H., Seibert, J., 2016a. Landscape controls on spatiotemporal discharge variability in a boreal catchment. Water Resour. Res. 52, 6541–6556. http://dx.doi.org/10.1002/2016WR019186.
Karlsen, R.H., Seibert, J., Grabs, T., Laudon, H., Blomkvist, P., Bishop, K., 2016b. The assumption of uniform specific discharge: unsafe at any time? Hydrol. Process. http://dx.doi.org/10.1002/hyp.10877.
Kim, J.-H., 2009. Estimating classification error rate: Repeated cross-validation, repeated hold-out and bootstrap. Comput. Stat. Data An. 53, 3735–3745. http://dx.doi.org/10.1016/j.csda.2009.04.009.
Kirilenko, A.P., Sedjo, R.A., 2007. Climate change impacts on forestry. Proc. Natl. Acad. Sci. U.S.A. 104, 19697–19702. http://dx.doi.org/10.1073/pnas.0701424104.
Kite, G.W., Kouwen, N., 1992. Watershed modeling using land classifications. Water Resour Res 28, 3193–3200. https://doi.org/Provider: John Wiley & Sons, Ltd Content:text/plain; charset = "UTF-8" TY - JOUR AU - Kite, G. W. AU - Kouwen, N. TI - Watershed modeling using land classifications JO - Water Resources Research JA - Water Resour. Res. VL - 28 IS - 12 SN - 1944-7973 UR - http://dx.doi.org/10.1029/92WR01819 DO - 10.1029/92WR01819 SP - 3193 EP - 3200 KW - 1860 Streamflow KW - 1866 Soil moisture PY - 1992 ER -
Klemeš, V., 1986. Operational testing of hydrological simulation models/Vérification, en conditions réelles, des modèles de simulation hydrologique. Hydrol. Sci. J. 31, 13–24. http://dx.doi.org/10.1080/02626668609491024.
Kohavi, R., 1995. A study of cross-validation and bootstrap for accuracy estimation and model selection. In: IJCAI'95 Proceedings of the 14th International Joint Conference on Artificial Intelligence – Volume 2. Presented at the International Joint Conference on Artificial Intelligence. Morgan Kaufmann Publishers Inc., San Francisco, CA, USA, Montreal, Canada, pp. 1137–1145.
Kokkonen, T.S., Jakeman, A.J., 2002. Chapter 14: structural effects of landscape and land use on streamflow response. In: Beck, M.B. (Ed.), Environmental Foresight and Models: A Manifesto. Elsevier, Oxford, UK, pp. 303–321.
Kotlarski, S., Keuler, K., Christensen, O.B., Colette, A., Déqué, M., Gobiet, A., Goergen, K., Jacob, D., Lüthi, D., van Meijgaard, E., Nikulin, G., Schär, C., Teichmann, C., Vautard, R., Warrach-Sagi, K., Wulfmeyer, V., 2014. Regional climate modeling on European scales: a joint standard evaluation of the EURO-CORDEX RCM ensemble. Geosci. Model Dev. 7, 1297–1333. http://dx.doi.org/10.5194/gmd-7-1297-2014.
Kottek, M., Grieser, J., Beck, C., Rudolf, B., Rubel, F., 2006. World map of the Koppen-Geiger climate classification updated. Meteorologische Zeitschrift 15, 259–264. http://dx.doi.org/10.1127/0941-2948/2006/0130.
Kunstmann, H., Schneider, K., Forkel, R., Knoche, R., 2004. Impact analysis of climate change for an Alpine catchment using high resolution dynamic downscaling of ECHAM4 time slices. Hydrol. Earth Syst. Sci. 8, 1030–1044. http://dx.doi.org/10.5194/hess-8-1031-2004.
Lacombe, G., Ribolzi, O., de Rouw, A., Pierret, A., Latsachak, K., Silvera, N., Pham Dinh, R., Orange, D., Janeau, J.-L., Soulileuth, B., Robain, H., Taccoen, A., Sengphaathith, P., Mouche, E., Sengtaheuanghoung, O., Tran Duc, T., Valentin, C., 2016. Contradictory hydrological impacts of afforestation in the humid tropics evidenced by long-term field monitoring and simulation modelling. Hydrol. Earth Syst. Sci. 20, 2691–2704. http://dx.doi.org/10.5194/hess-20-2691-2016.
Ladson, A.R., Brown, R., Neal, B., Nathan, R., 2013. A standard approach to baseflow separation using the Lyne and Hollick filter. Austr. J. Water Res. 17, 25. http://dx.doi.org/10.7158/W12-028.2013.17.1.
Lake, P.S., 2003. Ecological effects of perturbation by drought in flowing waters. Freshwater Biol. 48, 1161–1172. http://dx.doi.org/10.1046/j.1365-2427.2003.01086.x.
Laudon, H., Buttle, J., Carey, S.K., McDonnell, J., McGuire, K., Seibert, J., Shanley, J., Soulsby, C., Tetzlaff, D., 2012. Cross-regional prediction of long-term trajectory of stream water DOC response to climate change. Geophys. Res. Lett. 39. http://dx.doi.org/10.1029/2012GL053033.
Laudon, H., Taberman, I., Ågren, A., Futter, M., Ottosson-Löfvenius, M., Bishop, K., 2013. The Krycklan Catchment Study—a flagship infrastructure for hydrology, biogeochemistry, and climate research in the boreal landscape. Water Resour. Res. 49, 7154–7158. http://dx.doi.org/10.1002/wrcr.20520.
Lendasse, A., Wertz, V., Verleysen, M., 2003. Model selection with cross-validations and bootstraps — application to time series prediction with RBFN models. In: Kaynak, O., Alpaydin, E., Oja, E., Xu, L. (Eds.), Artificial Neural Networks and Neural Information Processing — ICANN/ICONIP 2003: Joint International Conference ICANN/ICONIP 2003 Istanbul, Turkey, June 26–29, 2003 Proceedings. Springer Berlin Heidelberg, Berlin, Heidelberg, pp. 573–580.
Ley, R., Casper, M.C., Hellebrand, H., Merz, R., 2011. Catchment classification by runoff behaviour with self-organizing maps (SOM). Hydrol. Earth Syst. Sci. 15, 2947–2962. http://dx.doi.org/10.5194/hess-15-2947-2011.
Lindström, G., Johansson, B., Persson, M., Gardelin, M., Bergström, S., 1997. Development and test of the distributed HBV-96 hydrological model. J. Hydrol. 201, 272–288. http://dx.doi.org/10.1016/S0022-1694(97)00041-3.
Lyne, V., Hollick, M., 1979. Stochastic time-variable rainfall-runoff modelling. In: Proceedings of the Hydrology and Water Resources Symposium. Presented at the Hydrology and Water Resources Symposium. Institution of Engineers National Conference Publication, Perth, Australia, pp. 89–92.
Lyon, S.W., Nathanson, M., Spans, A., Grabs, T., Laudon, H., Temnerud, J., Bishop, K.H., Seibert, J., 2012. Specific discharge variability in a boreal landscape. Water Resour. Res. 48. http://dx.doi.org/10.1029/2011WR011073.
Mao, D., Cherkauer, K.A., 2009. Impacts of land-use change on hydrologic responses in the Great Lakes region. J. Hydrol. 374, 71–82. http://dx.doi.org/10.1016/j.jhydrol.2009.06.016.
McGlynn, B., McDonnell, J., Stewart, M., Seibert, J., 2003. On the relationships between catchment scale and streamwater mean residence time. Hydrol. Process. 17, 175–181. http://dx.doi.org/10.1002/hyp.5085.
McVicar, T.R., Roderick, M.L., Donohue, R.J., Li, L.T., Van Niel, T.G., Thomas, A., Grieser, J., Jhajharia, D., Himri, Y., Mahowald, N.M., Mescherskaya, A.V., Kruger, A.C., Rehman, S., Dinpashoh, Y., 2012. Global review and synthesis of trends in observed terrestrial near-surface wind speeds: implications for evaporation. J. Hydrol. 416–417, 182–205. http://dx.doi.org/10.1016/j.jhydrol.2011.10.024.
Mendoza, P.A., Clark, M.P., Mizukami, N., Newman, A.J., Barlage, M., Gutmann, E.D., Rasmussen, R.M., Rajagopalan, B., Brekke, L.D., Arnold, J.R., 2015. Effects of hydrologic model choice and calibration on the portrayal of climate change impacts. J. Hydrometeorol. 16, 762–780. http://dx.doi.org/10.1175/JHM-D-14-0104.1.
Mengis, N., Keller, D.P., Eby, M., Oschlies, A., 2015. Uncertainty in the response of transpiration to CO_2 and implications for climate change. Environ. Res. Lett. 10, 094001. http://dx.doi.org/10.1088/1748-9326/10/9/094001.
Merz, R., Blöschl, G., 2004. Regionalisation of catchment model parameters. J. Hydrol. 287, 95–123. http://dx.doi.org/10.1016/j.jhydrol.2003.09.028.
Milad, M., Schaich, H., Konold, W., 2013. How is adaptation to climate change reflected in current practice of forest management and conservation? A case study from Germany. Biodivers. Conserv. 22, 1181–1202. http://dx.doi.org/10.1007/s10531-012-0337-8.
Milly, P.C.D., Dunne, K.A., Vecchia, A.V., 2005. Global pattern of trends in streamflow and water availability in a changing climate. Nature 438, 347–350. http://dx.doi.org/10.1038/nature04312.
Monteith, J.L., 1965. Evaporation and environment. Symp. Soc. Exp. Biol. 19, 205–234.
Muerth, M.J., Gauvin St-Denis, B., Ricard, S., VelÃ¡zquez, J.A., Schmid, J., Minville, M., Caya, D., Chaumont, D., Ludwig, R., Turcotte, R., 2013. On the need for bias correction in regional climate scenarios to assess climate change impacts on river runoff. Hydrol. Earth Syst. Sci. 17, 1189–1204. http://dx.doi.org/10.5194/hess-17-1189-2013.
Musau, J., Sang, J., Gathenya, J., Luedeling, E., 2015. Hydrological responses to climate change in Mt. Elgon watersheds. J. Hydrol. Reg. Stud. 3, 233–246. http://dx.doi.org/10.1016/j.ejrh.2014.12.001.
Nagelkerke, N.J.D., 1991. A note on a general definition of the coefficient of determination. Biometrika 78, 691–692. http://dx.doi.org/10.2307/2337038.
Nakicenovic, N., Alcamo, J., Davis, G., de Vries, B., Fenhann, J., Gaffin, S., Gregory, K., Grübler, A., Jung, T.Y., Kram, T., Dadi, Z., 2000. IPCC Special Report on Emissions Scenarios. Cambridge University Press, Cambridge, UK.
Nash, J.E., Sutcliffe, J.V., 1970. River flow forecasting through conceptual models part I - a discussion of principles. J. Hydrol. 10, 282–290. http://dx.doi.org/10.1016/0022-1694(70)90255-6.
Nathan, R.J., McMahon, T.A., 1990. Evaluation of automated techniques for base flow and recession analyses. Water Resour. Res. 26, 1465–1473. http://dx.doi.org/10.1029/WR026i007p01465.
Nijssen, B., O'Donnell, G.M., Hamlet, A.F., Lettenmaier, D.P., 2001. Hydrologic sensitivity of global rivers to climate change. Clim. Change 50, 143–175. http://dx.doi.org/10.1023/A:1010616428763.
Ochoa-Tocachi, B.F., Buytaert, W., De Bièvre, B., 2016. Regionalization of land-use impacts on streamflow using a network of paired catchments: regionalization using paired catchments. Water Resour. Res. 52, 6710–6729. http://dx.doi.org/10.1002/2016WR018596.
Oni, S.K., Tiwari, T., Ledesma, J.L.J., Ågren, A.M., Teutschbein, C., Schelker, J., Laudon, H., Futter, M.N., 2015. Local- and landscape-scale impacts of clear-cuts and climate change on surface water dissolved organic carbon in boreal forests. J. Geophys. Res.-Biogeo 120. http://dx.doi.org/10.1002/2015JG003190.
Patil, S., Stieglitz, M., 2012. Controls on hydrologic similarity: role of nearby gauged catchments for prediction at an ungauged catchment. Hydrol. Earth Syst. Sci. 16, 551–562. http://dx.doi.org/10.5194/hess-16-551-2012.
Pearson, K., 1920. Notes on the history of correlation. Biometrika 13, 25. http://dx.doi.org/10.2307/2331722.
Peña-Arancibia, J.L., van Dijk, A.I.J.M., Mulligan, M., Bruijnzeel, L.A., 2010. The role of climatic and terrain attributes in estimating baseflow recession in tropical catchments. Hydrol. Earth Syst. Sci. 14, 2193–2205. http://dx.doi.org/10.5194/hess-14-2193-2010.
Peña-Arancibia, J.L., Zhang, Y., Pagendam, D.E., Viney, N.R., Lerat, J., van Dijk, A.I.J.M., Vaze, J., Frost, A.J., 2015. Streamflow rating uncertainty: characterisation and impacts on model calibration and performance. Environ. Modell. Softw. 63, 32–44. http://dx.doi.org/10.1016/j.envsoft.2014.09.011.
Persson, H., Fransson, J., 2014. Forest variable estimation using radargrammetric processing of TerraSAR-X images in boreal forests. Remote Sens. 6, 2084–2107. http://dx.doi.org/10.3390/rs6032084.
Petersen-Øverleir, A., 2004. Accounting for heteroscedasticity in rating curve estimates. J. Hydrol. 292, 173–181. http://dx.doi.org/10.1016/j.jhydrol.2003.12.024.
Pinay, G., Peiffer, S., De Dreuzy, J.-R., Krause, S., Hannah, D.M., Fleckenstein, J.H., Sebilo, M., Bishop, K., Hubert-Moy, L., 2015. Upscaling nitrogen removal capacity from local hotspots to low stream orders' drainage basins. Ecosystems 18, 1101–1120. http://dx.doi.org/10.1007/s10021-015-9878-5.
Pool, S., Vis, M.J.P., Knight, R.R., Seibert, J., 2017. Streamflow characteristics from modeled runoff time series – importance of calibration criteria selection. Hydrol. Earth Syst. Sci. 21, 5443–5457. http://dx.doi.org/10.5194/hess-21-5443-2017.
Post, D.A., Jakeman, A.J., 1999. Predicting the daily streamflow of ungauged catchments in SE Australia by regionalising the parameters of a lumped conceptual rainfall-runoff model. Ecol. Modell. 123, 91–104. http://dx.doi.org/10.1016/S0304-3800(99)00125-8.
Rytter, L., Johansson, K., Karlsson, B., Stener, L.-G., 2013. Tree species, genetics and regeneration for bioenergy feedstock in Northern Europe. In: Kellomäki, S., Kilpeläinen, A., Alam, A. (Eds.), Forest BioEnergy Production: Management, Carbon

Sequestration and Adaptation. Springer Science+Business Media, New York, USA, pp. 7–37.
Sahin, V., Hall, M.J., 1996. The effects of afforestation and deforestation on water yields. J. Hydrol. 178, 293–309. http://dx.doi.org/10.1016/0022-1694(95)02825-0.
Samaniego, L., Bárdossy, A., Kumar, R., 2010. Streamflow prediction in ungauged catchments using copula-based dissimilarity measures. Water Resour. Res. 46, 1–22. http://dx.doi.org/10.1029/2008WR007695.
Sawicz, K., Wagener, T., Sivapalan, M., Troch, P.A., Carrillo, G., 2011. Catchment classification: empirical analysis of hydrologic similarity based on catchment function in the eastern USA. Hydrol. Earth Syst. Sci. 15, 2895–2911. http://dx.doi.org/10.5194/hess-15-2895-2011.
Schelker, J., Kuglerová, L., Eklöf, K., Bishop, K., Laudon, H., 2013. Hydrological effects of clear-cutting in a boreal forest – snowpack dynamics, snowmelt and streamflow responses. J. Hydrol. 484, 105–114. http://dx.doi.org/10.1016/j.jhydrol.2013.01.015.
Schoonover, J.E., Lockaby, B.G., Helms, B.S., 2006. Impacts of land cover on stream hydrology in the West Georgia Piedmont, USA. J. Environ. Qual. 35, 2123–2131.
Seibert, J., 2005. HBV Manual 2005.
Seibert, J., 2000. Multi-criteria calibration of a conceptual runoff model using a genetic algorithm. Hydrol. Earth Syst. Sci. 4, 215–224. http://dx.doi.org/10.5194/hess-4-215-2000.
Seibert, J., 1999. Regionalisation of parameters for a conceptual rainfall-runoff model. Agr. Forest. Meteorol. 98–99, 279–293. http://dx.doi.org/10.1016/S0168-1923(99)00105-7.
Seibert, J., Bishop, K.H., Nyberg, L., 1997. A test of TOPMODEL's ability to predict spatially distributed groundwater levels. Hydrol. Process. 11, 1131–1144. http://dx.doi.org/10.1002/(sici)1099-1085(199707)11:9<1131::aid-hyp549>3.0.co;2-#.
Seibert, J., Vis, M.J.P., 2012. Teaching hydrological modeling with a user-friendly catchment-runoff-model software package. Hydrol. Earth Syst. Sci. 16, 3315–3325. http://dx.doi.org/10.5194/hess-16-3315-2012.
Seyfried, M.S., Wilcox, B.P., 1995. Scale and the nature of spatial variability: field examples having implications for hydrologic modeling. Water Resour. Res. 31, 173–184. http://dx.doi.org/10.1029/94WR02025.
Shamir, E., Imam, B., Gupta, H.V., Sorooshian, S., 2005. Application of temporal streamflow descriptors in hydrologic model parameter estimation. Water Resour. Res. 41, W06021. http://dx.doi.org/10.1029/2004WR003409.
Shaw, S.B., Riha, S.J., 2011. Assessing temperature-based PET equations under a changing climate in temperate, deciduous forests. Hydrol. Process. 25, 1466–1478. http://dx.doi.org/10.1002/hyp.7913.
Sivapalan, M., 2005. Pattern, process and function: elements of a unified theory of hydrology at the catchment scale,. In: Anderson, M.G. (Ed.), Encyclopedia of Hydrological Sciences. John Wiley & Sons, Ltd, pp. 193–219.
Sivapalan, M., 2003. Prediction in ungauged basins: a grand challenge for theoretical hydrology. Hydrol. Process. 17, 3163–3170. http://dx.doi.org/10.1002/hyp.5155.
Sivapalan, M., Takeuchi, K., Franks, S.W., Gupta, V.K., Karambiri, H., Lakshmi, V., Liang, X., McDonnell, J.J., Mendiondo, E.M., O'Connell, P.E., Oki, T., Pomeroy, J.W., Schertzer, D., Uhlenbrook, S., Zehe, E., 2003. IAHS Decade on Predictions in Ungauged Basins (PUB), 2003–2012: shaping an exciting future for the hydrological sciences. Hydrol. Sci. J. 48, 857–880. http://dx.doi.org/10.1623/hysj.48.6.857.51421.
SLU, 2015. Forest statistics 2015, Official Statistics of Sweden. Swedish University of Agricultural Sciences (SLU), Umeå, Sweden.
Spearman, C., 1904. The proof and measurement of association between two things. Am. J. Psychol. 15, 72–101. http://dx.doi.org/10.1093/ije/dyq191.
Stahl, K., Tallaksen, L.M., Gudmundsson, L., Christensen, J.H., 2011. Streamflow data from small basins: a challenging test to high-resolution regional climate modeling. J. Hydrometeorol. 12, 900–912. http://dx.doi.org/10.1175/2011JHM1356.1.
Surfleet, C.G., Tullos, D., Chang, H., Jung, I.-W., 2012. Selection of hydrologic modeling approaches for climate change assessment: a comparison of model scale and structures. J. Hydrol. 464–465, 233–248. http://dx.doi.org/10.1016/j.jhydrol.2012.07.012.
Taylor, K.E., 2001. Summarizing multiple aspects of model performance in a single diagram. J. Geophys. Res.-Atmos. 106, 7183–7192. http://dx.doi.org/10.1029/2000JD900719.
Tetzlaff, D., Waldron, S., Brewer, M.J., Soulsby, C., 2007. Assessing nested hydrological and hydrochemical behaviour of a mesoscale catchment using continuous tracer data. J. Hydrol. 336, 430–443. http://dx.doi.org/10.1016/j.jhydrol.2007.01.020.
Teutschbein, C., Grabs, T., Karlsen, R.H., Laudon, H., Bishop, K., 2015. Hydrological response to changing climate conditions: spatial streamflow variability in the boreal region. Water Resour. Res. 51, 9425–9446. http://dx.doi.org/10.1002/2015WR017337.
Teutschbein, C., Seibert, J., 2013. Is bias correction of regional climate model (RCM) simulations possible for non-stationary conditions? Hydrol. Earth Syst. Sci. 17, 5061–5077. http://dx.doi.org/10.5194/hess-17-5061-2013.
Teutschbein, C., Seibert, J., 2012. Bias correction of regional climate model simulations for hydrological climate-change impact studies: review and evaluation of different methods. J. Hydrol. 456–457, 12–29. http://dx.doi.org/10.1016/j.jhydrol.2012.05.052.
Teutschbein, C., Seibert, J., 2010. Regional climate models for hydrological impact studies at the catchment scale: a review of recent modeling strategies. Geogr. Compass 4, 834–860. http://dx.doi.org/10.1111/j.1749-8198.2010.00357.x.
Teutschbein, C., Sponseller, R.A., Grabs, T., Blackburn, M., Boyer, E.W., Bishop, K., 2016. An ensemble approach to assess the effects of climate change on riverine inorganic nitrogen loading in Sweden. Global Biogeochem Cy In review.
Teutschbein, C., Wetterhall, F., Seibert, J., 2011. Evaluation of different downscaling techniques for hydrological climate-change impact studies at the catchment scale. Clim. Dynam. 37, 2087–2105. http://dx.doi.org/10.1007/s00382-010-0979-8.
The National Academy of Sciences, 2008. Hydrologic Effects of a Changing Forest Landscape, Report in Brief. Washington, D.C., USA.
Tomkins, K.M., 2014. Uncertainty in streamflow rating curves: methods, controls and consequences. Hydrol. Process. 28, 464–481. http://dx.doi.org/10.1002/hyp.9567.
Tong, S.T.Y., Sun, Y., Ranatunga, T., He, J., Yang, Y.J., 2012. Predicting plausible impacts of sets of climate and land use change scenarios on water resources. Appl. Geogr. 32, 477–489. http://dx.doi.org/10.1016/j.apgeog.2011.06.014.
Toth, E., 2013. Catchment classification based on characterisation of streamflow and precipitation time series. Hydrol. Earth Syst. Sci. 17, 1149–1159. http://dx.doi.org/10.5194/hess-17-1149-2013.
Trancoso, R., Larsen, J.R., McAlpine, C., McVicar, T.R., Phinn, S., 2016. Linking the Budyko framework and the Dunne diagram. J. Hydrol. 535, 581–597. http://dx.doi.org/10.1016/j.jhydrol.2016.02.017.
Trancoso, R., Larsen, J.R., McVicar, T.R., Phinn, S.R., McAlpine, C.A., 2017. CO2-vegetation feedbacks and other climate changes implicated in reducing base flow. Geophys. Res. Lett. http://dx.doi.org/10.1002/2017GL072759.
Ukkola, A.M., Prentice, I.C., Keenan, T.F., van Dijk, A.I.J.M., Viney, N.R., Myneni, R.B., Bi, J., 2015. Reduced streamflow in water-stressed climates consistent with CO2 effects on vegetation. Nat. Clim. Change 6, 75–78. http://dx.doi.org/10.1038/nclimate2831.
Van der Linden, P., Mitchell, J.F.B., 2009. ENSEMBLES: Climate Change and Its Impacts: Summary of Research and Results from the ENSEMBLES Project. Met Office Hadley Centre, Exeter, UK.
van Dijk, A.I.J.M., Hairsine, P.B., Arancibia, J.P., Dowling, T.I., 2007. Reforestation, water availability and stream salinity: a multi-scale analysis in the Murray-Darling Basin, Australia. Forest Ecol. Manag. 251, 94–109. http://dx.doi.org/10.1016/j.foreco.2007.06.012.
Wagener, T., Sivapalan, M., Troch, P., Woods, R., 2007. Catchment classification and hydrologic similarity. Geogr. Compass 1, 901–931. http://dx.doi.org/10.1111/j.1749-8198.2007.00039.x.
Westerberg, I.K., Wagener, T., Coxon, G., McMillan, H.K., Castellarin, A., Montanari, A., Freer, J., 2016. Uncertainty in hydrological signatures for gauged and ungauged catchments. Water Resour. Res. 52, 1847–1865. http://dx.doi.org/10.1002/2015WR017635.
Wild, M., 2009. Global dimming and brightening: a review. J. Geophys. Res. 114. http://dx.doi.org/10.1029/2008JD011470.
Willett, K.M., Jones, P.D., Gillett, N.P., Thorne, P.W., 2008. Recent changes in surface humidity: development of the HadCRUH dataset. J. Clim. 21, 5364–5383. http://dx.doi.org/10.1175/2008JCLI2274.1.
Williams, C.J., McNamara, J.P., Chandler, D.G., 2009. Controls on the temporal and spatial variability of soil moisture in a mountainous landscape: the signature of snow and complex terrain. Hydrol. Earth Syst. Sci. 13, 1325–1336. http://dx.doi.org/10.5194/hess-13-1325-2009.
Willmott, C.J., Ackleson, S.G., Davis, R.E., Feddema, J.J., Klink, K.M., Legates, D.R., O'Donnell, J., Rowe, C.M., 1985. Statistics for the evaluation and comparison of models. J. Geophys. Res. 90, 8995–9005. http://dx.doi.org/10.1029/JC090iC05p08995.
Wood, P.J., Armitage, P.D., 1997. Biological effects of fine sediment in the lotic environment. Environ. Manage. 21, 203–217. http://dx.doi.org/10.1007/s002679900019.
Xu, C.Y., Singh, V.P., 2001. Evaluation and generalization of temperature-based methods for calculating evaporation. Hydrol. Process. 15, 305–319. http://dx.doi.org/10.1002/hyp.119.
Yadav, M., Wagener, T., Gupta, H., 2007. Regionalization of constraints on expected watershed response behavior for improved predictions in ungauged basins. Adv. Water Resour. 30, 1756–1774. http://dx.doi.org/10.1016/j.advwatres.2007.01.005.
Yang, Y., Donohue, R.J., McVicar, T.R., Roderick, M.L., Beck, H.E., 2016. Long-term CO2 fertilization increases vegetation productivity and has little effect on hydrological partitioning in tropical rainforests. J. Geophys. Res.-Biogeo 121, 2125–2140. http://dx.doi.org/10.1002/2016JG003475.
Yilmaz, K.K., Gupta, H.V., Wagener, T., 2008. A process-based diagnostic approach to model evaluation: application to the NWS distributed hydrologic model. Water Resour. Res. 44, W09417. http://dx.doi.org/10.1029/2007WR006716.
Zhang, L., Dawes, W.R., Walker, G.R., 2001. Response of mean annual evapotranspiration to vegetation changes at catchment scale. Water Resour. Res. 37, 701–708. http://dx.doi.org/10.1029/2000WR900325.
Zhang, M., Liu, N., Harper, R., Li, Q., Liu, K., Wei, X., Ning, D., Hou, Y., Liu, S., 2017. A global review on hydrological responses to forest change across multiple spatial scales: importance of scale, climate, forest type and hydrological regime. J. Hydrol. 546, 44–59. http://dx.doi.org/10.1016/j.jhydrol.2016.12.040.
Zhang, S., Yang, Y., McVicar, T.R., Yang, D., 2018. An analytical solution for the impact of vegetation changes on hydrological partitioning within the budyko framework. Water Resour. Res. 54, 519–537. http://dx.doi.org/10.1002/2017WR022028.
Zhang, Y.-K., Schilling, K.E., 2006. Increasing streamflow and baseflow in Mississippi River since the 1940s: effect of land use change. J. Hydrol. 324, 412–422. http://dx.doi.org/10.1016/j.jhydrol.2005.09.033.